Cross-kingdom anti-inflammatory effects of fungal melanin on airway epithelium by post-translational blockade of chemokine secretion

Jennifer L. Reedy[1,2], Arianne J. Crossen[1], Rebecca A. Ward[1], Christopher M. Reardon[1], Hannah Brown Harding[1,2], Kyle J. Basham[1], Jayaraj Rajagopal[3,4,5,6], Jatin M. Vyas[1,2,*]

[1] Department of Medicine, Division of Infectious Diseases, Massachusetts General Hospital, Boston, MA, 02114, USA

[2] Harvard Medical School, Boston, MA, 02115, USA

[3] Center for Regenerative Medicine, Massachusetts General Hospital, Boston, MA, 02114, USA

[4] Division of Pulmonary and Critical Care Medicine, Department of Medicine, Massachusetts General Hospital, Boston, MA, 02114, USA

[5] Harvard Stem Cell Institute, Cambridge, MA, 02138, USA

[6] Klarman Cell Observatory, Broad Institute of Massachusetts Institute of Technology and Harvard, Cambridge, MA, 02142, USA

*Correspondence: jvyas@mgh.harvard.edu

Summary

Respiratory infections caused by the human fungal pathogens, *Aspergillus fumigatus* and *Cryptococcus neoformans*, are a major cause of mortality for immunocompromised patients. Exposure to these pathogens occurs through inhalation, although the role of the respiratory epithelium in disease pathogenesis has not been defined. Employing a primary human airway epithelial model, we demonstrate that fungal melanins potently block the post-translational secretion of CXCL1 and CXCL8 independent of transcription or the requirement of melanin to be phagocytosed, leading to a significant reduction of neutrophils to the apical airway both *in vitro* and *in vivo*. *Aspergillus*-derived melanin, a major constituent of the fungal cell wall, has far-reaching effects, dampening airway epithelial chemokine production in response to fungi, bacteria, and exogenous cytokines. Taken together, our results reveal a critical role for melanin

interaction with airway epithelium in shaping the host response to fungal and bacterial pathogens.

Keywords: airway epithelium, *Aspergillus*, melanin, innate immunity, host-pathogen interaction, fungal immunology

Introduction

Aspergillus fumigatus is the most prominent respiratory fungal pathogen and causes a spectrum of clinical manifestations ranging from allergic disease to severe invasive infections. Despite the ubiquity of this fungal pathogen in the environment, only ~10% of immunocompromised patients (*e.g.,* neutropenic or allogenic bone marrow transplant recipients) develop invasive aspergillosis (IA), indicating that other factors play a significant role in determining the true risk for this infection[1]. In addition to infection associated with the immunocompromised state, there is an increased risk of IA following pulmonary viral infections (*e.g.,* influenza, SARS-CoV-2) and in those with underlying lung disease (*e.g.,* asthma, cystic fibrosis [CF], chronic obstructive pulmonary disease [COPD])[2-5]. The mortality from *Aspergillus*-related pulmonary disease remains unacceptably high (>50%), coinciding with elevated rates of *Aspergillus* multidrug resistance[6-8]. Despite this, there is a void in our understanding of the mechanistic interactions governing the invasion of *Aspergillus* at its first point of contact with the host, the airway epithelium.

In immune cells, activation of pattern recognition receptors (PRRs), such as the C-type lectin receptor (CLRs), Toll-like receptors (TLRs), NOD-like receptors (NLRs), and Rig-I-like receptors, mediate fungal recognition of cell wall components and subsequent host responses[9]. The cell wall of *Aspergillus* is primarily composed of polysaccharides, including galactosaminogalactan, galactomannan, β-1,3 glucan, β-1,4 glucan, and chitin. Most humans are exposed to *Aspergillus* through the inhalation of conidia, the reproductive propagules of the fungus, which range from 2-3 µm in size and are easily aerosolized in the environment. In addition to the typical cell wall components, *Aspergillus* conidia are surrounded by a hydrophobic rodlet and 1,8-dihydroxy naphthalene (DHN) melanin layers[10,11]. Once inhaled by the host, conidia swell and shed these outer layers, exposing the carbohydrate matrix of the cell wall. In immune cells, fungal melanin possesses the remarkable capacity to absorb reactive

oxygen species (ROS) and blunt pro-inflammatory cascades, serving as a key virulence factor for many pathogens, including *Aspergillus*[12-17]. Amelanotic strains of clinically relevant fungal pathogens lose their capacity to mount successful infections in mammalian host model systems, indicating that melanin plays a key and non-redundant role in virulence. Indeed, the presence of melanized *Aspergillus* leads to blockage of the phagosome biogenesis[18] and removal of the melanin in the phagosome reprograms macrophage metabolism, promoting an antifungal response[19].

Clinical data and current literature indicate that several immune system components are critical for the recognition and swift clearance of fungal pathogens. Still, the rules governing the inflammatory responses to fungi in the lungs are poorly understood. Past studies have focused on innate and adaptive immune cells but have often overlooked a key player in respiratory infections: the airway epithelium - the primary point of contact for inhaled conidia[20-23]. The conducting airways are sites of *Aspergillus* colonization and invasion[20-23]. Fortunately, *in vitro* differentiation of primary airway basal cells recapitulates the true diversity of conducting airway epithelium with all of the relevant common (basal, ciliated, club, goblet) and rare (ionocytes, tuft, neuroendocrine) cell types in pseudostratified layers, enabling mechanistic studies in rare populations and the epithelial network in disease[24]. Additionally, these cells form polarized barriers and enable the investigation of basolateral and apical epithelial responses when grown at air-liquid interface (ALI)[25,26]. While the primary human airway epithelial cell (hAEC) ALI model may not fully recapitulate the *in vivo* environment (*e.g.,* lacks resident immune cells, endothelial cells, fibroblasts), this model offers the advantages of a highly pliable system to conduct mechanistic studies without compromising relevant human physiology[26-28] and allow us to pinpoint mechanisms specific to the interaction of the epithelium and inhaled conidia where the microbe first encounters host defense. In addition to utilizing this system, we also use the airway epithelial cell line H292, a mucoepitheliod non-small cell lung carcinoma cell line, which has

previously been used extensively in modeling airway epithelial responses to bacterial pathogens. While this cell line does not capture the cellular diversity of the airway epithelium, it is well-suited to mechanistic studies due to cellular uniformity. We previously demonstrated a role for melanin in immune response to *Aspergillus fumigatus* orchestrated by airway epithelium using both primary hAEC and H292 epithelial models[26]. We observed that airway epithelium infected with *A. fumigatus* lacking DHN melanin promoted greater transepithelial migration of neutrophils than wildtype conidia. The mechanism by which melanin modulates epithelial-mediated neutrophil transmigration remains unknown.

In the present study, we leveraged primary hAEC to demonstrate that purified fungal melanin at the apical surface of epithelial cells blocked migration of neutrophils and blunted the apical secretion of chemoattractant chemokines. We determined that DHN melanin suppression of neutrophil transmigration and chemokines occured in response to both fungal and bacterial pathogens. Furthermore, L-DOPA melanin from *Cryptococcus neoformans* and other commercially available synthetic melanins inhibited CXLC8 (also known as IL-8) secretion, showing these effects were not unique to DHN melanin, but rather is a preserved property of fungal melanins. We determined that fungal melanin abolished the apical-basolateral CXCL8 gradient as a mechanism to block neutrophil recruitment. Lastly, we demonstrated that melanin suppressed secretion, but not translation or transcription, of CXCL8 in airway epithelium in a phagocytosis-independent manner. Together, these data indicated that fungal melanin inhibits epithelial-mediated inflammation through blocking the secretion of critical pro-inflammatory chemokines.

Results

Aspergillus ***melanin inhibits transepithelial migration of primary neutrophils***

We previously demonstrated that hAEC induce neutrophil transmigration upon stimulation with *A. fumigatus* wildtype conidia[26]. However, induction of neutrophil transmigration required at least 4h of infection with *A. fumigatus* in contrast to the bacterial pathogen, *Pseudomonas aeruginosa*, which induced robust neutrophil transmigration within 1h[26]. Furthermore, *Aspergillus* conidia that lacked the ability to produce DHN melanin (*ΔpksP*) induced neutrophil transmigration within 1h of infection similarly to *P. aeruginosa*, suggesting that melanin was blocking hAEC responses to resting conidia[26]. Thus, we hypothesized that melanin could act via two mechanisms to block neutrophil migration: melanin could actively downregulate pro-inflammatory responses or serve as a passive barrier to prevent host access to immunostimulatory epitopes on the fungal cell wall. To test these hypotheses, we performed mixing studies with *A. fumigatus* melanin ghosts and amelanotic *ΔpksP* conidia. Creation of melanin ghosts is a well-described technique in which melanized conidia are biochemically and enzymatically degraded to strip all cellular components except a rigid shell of purified melanin resembling the original size and shape of the conidia[18,29-33]. To ascertain whether melanin coating of conidia was required for its inhibitory function, we stimulated primary hAEC with *ΔpksP* conidia alone or in combination with melanin ghosts at a ratio of 5:1 melanin ghosts to *ΔpksP* conidia then measured neutrophil recruitment across the epithelium. Stimulation of hAEC with *ΔpksP* conidia mixed with melanin ghosts dampened neutrophil transmigration when compared to *ΔpksP* alone (**Figure 1A**). As expected melanin ghosts alone did not stimulate neutrophil transmigration.

We next examined if this response seen in primary hAEC extended to the human lung epithelial cell line, H292, which is routinely used to dissect airway responsiveness to bacterial pathogens[34-36]. While these cells do not recapitulate the cellular diversity of the primary airway epithelium, they are well suited to mechanistic studies given their homogeneity, thus we wished to determine if our phenotype could translate to this model system. We observed that infection

with *ΔpksP* conidia alone induced more neutrophil recruitment across H292 monolayers compared with *ΔpksP* conidia in the presence of melanin ghosts (**Figure 1B**) recapitulating the primary hAECs findings. Since the melanin in these experiments was applied as discrete particles that are unable to coat the surface of the *ΔpksP* conidia, these results indicate a model where melanin actively downregulates inflammatory responses rather than acting as a passive barrier on the surface of the conidia.

Aspergillus *melanin inhibits airway epithelial-derived CXCL8 and CXCL1*

To understand the mechanism of how neutrophil transmigration was silenced, we performed a Luminex assay using primary human airway epithelium derived from three healthy human donors. Primary hAEC was differentiated at ALI for 16 days prior to stimulation with either media alone (HBSS), *P. aeruginosa* (positive control), three wildtype strains of *A. fumigatus* (CEA10, Af293, B5233), or the amelanotic *A. fumigatus ΔpksP* strain (derived from B5233). CXCL8 and CXCL1 (also known as GROα) are two neutrophil chemoattractants produced by the airway epithelium and were the most abundant chemokines specifically induced by the mutant *ΔpksP A. fumigatus* strain, but not by wildtype strains (**Figure 2A-B**). We confirmed this difference in cytokine expression in H292 cells using both the *ΔpksP* and *ΔpksP* complemented strains (**Figure 2C-D**) to validate the use of these cells for mechanistic studies.

To determine if melanin acted through a blockade of epithelial chemokine secretion, we performed mixing studies in which we stimulated with a fixed concentration of *ΔpksP* conidia combined with graded amounts of melanin ghosts. The mixing assay revealed that the addition of melanin ghosts suppressed both CXCL8 and CXCL1 chemokine production in a dose-dependent manner (**Figures 2E-F**). Melanin ghosts alone applied at the highest concentration did not induce chemokine production.

The inhibitory effects of* Aspergillus *melanin extend to other pro-inflammatory stimuli

Thus far, our experiments suggested that melanin was not acting as a passive protective shield, but directly downregulated pro-inflammatory responses. We next sought to determine if fungal melanin anti-inflammatory actions were specific to fungal pathogens or if they represented a more general host-microbe interaction. *P. aeruginosa* is an important bacterial respiratory pathogen frequently found in co-infections with *A. fumigatus* in patients with CF. Therefore, we examined whether *Aspergillus* melanin ghosts could dampen *P. aeruginosa*-induced airway epithelial inflammation. We infected H292 monolayers with *P. aeruginosa* alone or in combination with melanin ghosts for 6h then quantified chemokine production. The addition of melanin ghosts suppressed CXCL8 (**Figures 3A**) and CXCL1 (**Figure S1A**) release in response to *P. aeruginosa* in a dose-dependent manner. To ensure that the melanin ghosts were not interfering with the ability of *P. aeruginosa* to bind to the epithelium, we confirmed that *P. aeruginosa* binding or internalization by the epithelial cells was not altered in the presence of melanin ghosts (**Figure S1B**), suggesting that the difference in chemokine production was not due to difference in the ability of *P. aeruginosa* to access the cells. Additionally, we performed an LDH cell viability assay that demonstrated no difference in cell viability in the presence of *Pseudomonas* with or without melanin (**Figure S1C**).

TNFα is a known inducer of airway epithelial CXCL8, therefore we hypothesized that melanin ghosts also blocks cytokine-induced CXCL8 in airway epithelial cells. We stimulated H292 epithelium with recombinant human TNFα for 6h in the presence of absence of melanin ghosts then quantified CXCL8 production in supernatants. The combination of melanin ghosts and TNFα stimulation of epithelial cells produced less CXCL8 compared to stimulation with TNFα alone (**Figure 3B**).

Melanin blocks* Pseudomonas*-induced transepithelial migration of neutrophils

Since co-stimulation of airway epithelium with *P. aeruginosa* and melanin ghosts resulted in a potent decrease of CXCL8 secretion, we examined the role of melanin ghosts in airway epithelial-induced neutrophils transmigration in response to *P. aeruginosa*. While CXCL8 is a known neutrophil chemoattractant that plays a role in epithelial-induced neutrophil transmigration[37,38], recruitment of neutrophils across the epithelium has been linked to other secreted compounds, such as hepoxilin A3, in response to *P. aeruginosa* [39-42]. We stimulated both primary hAEC and H292 with *P. aeruginosa* alone or in combination with melanin ghosts and quantified neutrophil transmigration using a myeloperoxidase assay. The addition of melanin ghosts decreased *P. aeruginosa*-induced neutrophil transmigration (**Figure 3C**), demonstrating that melanin blocked all mediators required for neutrophil recruitment to *Pseudomonas*.

To determine if the diminished transmigration of neutrophils also occurred *in vivo*, we infected mice with *P. aeruginosa* alone or in combination with melanin ghosts. *P. aeruginosa* induced neutrophil recruitment into the airways of mice, however the number of neutrophils in the bronchoalveolar lavage fluid was decreased in the presence of melanin (**Figure 3D**). Together, these data indicated that modulation of pro-inflammatory processes by melanin ghosts extends to recruitment of neutrophils to the site of infection.

Structurally distinct melanins from diverse sources block airway epithelial CXCL8 expression

Melanins are darkly pigmented molecules created through the polymerization of phenol or indole precursors forming polymers of high molecular weight[43,44]. Despite the ubiquity of melanin pigments across kingdoms (*e.g.,* animals, fungi, insects, helminths), the structure of melanin remains poorly defined. *Aspergillus* and dematiaceous molds produces DHN melanin catalyzed

by the polyketide synthase pathway[13-15,45]. However, some fungal pathogens such as *C. neoformans*, an environmental yeast that causes human infections including pneumonia and meningitis, contain melanin derived from L-tyrosine or L-dihydroxyphenylalanine (L-DOPA) produced through the action of tyrosinases[29,30,46-51]. L-DOPA/tyrosine-based melanins are structurally distinct from *Aspergillus* DHN melanin. This structural differences impact host responses as demonstrated by the recognition of DHN, but not L-DOPA, melanin by the CLR, MelLec or Clec1A, identified on human endothelial and immune cells[52]. To determine if the ability to inhibit the appearance of epithelial-derived CXCL8 in the supernatant was specific to *Aspergillus* DHN melanin, we utilized both *C. neoformans* melanin ghosts and a synthetic tyrosine-based melanin. As strong inducers of epithelial CXCL8, *Pseudomonas* and amelanotic *ΔpksP A. fumigatus* were used to stimulate H292 epithelium in the presence or absence of *C. neoformans* melanin ghosts. Similar to *Aspergillus* melanin ghosts, *Cryptococcus* melanin ghosts suppressed CXCL8 in the supernatant (**Figure 4A**).

In addition to our *C. neoformans* melanin ghosts, we also tested epithelial responses to a synthetic source of tyrosine-derived melanin. We previously created fungal-like particles (FLP) using purified fungal carbohydrates which associated with amine-coated polystyrene 3 μM microspheres using either chemical conjugation or adsorption[53,54]. Using this technique, we coated beads to create FLP with synthetic L-DOPA and β-1,3 glucan. β-1,3-glucan is a pro-inflammatory carbohydrate found in most fungal cell walls and was added as an additional control to demonstrate that any effect was due to the melanin and not a result of any coating applied to the microspheres. We stimulated H292 monolayers with *P. aeruginosa* either alone or in combination with unmodified FLP (naked beads), L-DOPA melanin-coated FLP, or β-1,3-glucan-coated FLP. We found that combined treatment with *P. aeruginosa* and L-DOPA-coated FLP led to a reduction in CXCL8 secretion, while no difference in CXCL8 secretion was observed when *P. aeruginosa* was combined with either unmodified FLP or β-1,3-glucan-coated

FLP (**Figure 4B**). Taken together, these results demonstrate that the immunomodulatory effect of melanin is not specific to *Aspergillus* melanin, but also occurs in response to *C. neoformans* L-DOPA based melanin and a synthetic tyrosine-based melanin.

Melanin abolishes the transepithelial gradient of CXCL8 required for neutrophil transmigration

Since epithelial cells are polarized, they secrete effector molecules selectively to either the apical or basolateral compartments or bidirectionally. Neutrophil transmigration to the apical surface (*i.e.* airway), requires the creation of a chemokine gradient established by differential secretion at the apical and basolateral surfaces[55-57]. To understand whether apical stimulation with melanin affected only apical chemokine production or both the apical and basolateral compartments, we stimulated H292 monolayers grown on Transwells with *P. aeruginosa* in the presence or absence of melanin ghosts and collected supernatants from both the apical and basolateral compartments. H292 were chosen to model this interactions because basolateral chemokine production by hAECs, even in the presence of *P. aeruginosa* was at the limit of detection. Stimulation with *P. aeruginosa* induced higher release of CXCL8 on the apical surface of the epithelium when compared to the basolateral surface (**Figure 5A**). The combination of *P. aeruginosa* with *Aspergillus* melanin ghosts significantly decreased both apical and basolateral CXCL8 production when epithelium compared with *Pseudomonas* alone. Furthermore, this co-stimulation effectively abolished the apical-basolateral chemokine gradient generated by *P. aeruginosa*.

Melanin induces durable impact on CXCL8 secretion

Thus far, our experiments examined the impact of melanin ghosts for short durations (6h or less). Thus, we sought to understand whether melanin stimulation of epithelium produced a

lasting effect at the epithelium or was a transient suppression of chemokine release. Melanin ghosts were durable and were not degraded in our cell culture systems (data not shown). We stimulated H292 epithelium with *P. aeruginosa* or TNFα in combination with melanin ghosts for 24h. After 24h stimulation, there was a persistent reduction of CXCL8 production by epithelial cells co-stimulated melanin ghosts compared with either *P. aeruginosa* or TNFα alone (**Figure 5B**), supporting the hypothesis that melanin silenced the airway epithelium to prevent inflammation, not simply delaying the initiation of response.

Melanin suppression of chemokine production is independent of phagocytosis of melanin or* de novo *transcription

To determine the mechanism by which melanin blocked CXCL8 production by airway epithelial cells, we first examined whether phagocytosis of melanin ghosts was required. H292 epithelium were pre-treated with cytochalasin D, an inhibitor of actin polymerization that effectively blocks phagocytosis, then stimulated with either TNFα alone or in combination with *Aspergillus* melanin ghosts. Melanin ghosts inhibited TNFα–induced CXCL8 production both in the presence and absence of cytochalasin D, suggesting that phagocytosis of melanin ghosts was not required for its anti-inflammatory action (**Figure 6A**).

We next investigated if melanin-induced transcription was required for CXCL8 suppression using the transcription inhibitor, actinomycin D. Following pre-treatments with vehicle control or actinomycin D, epithelial cells were incubated with TNFα, TNFα plus *Aspergillus* melanin ghosts, or melanin ghosts alone. TNFα induction of CXCL8 required CXCL8 transcription, therefore as expected addition of actinomycin D blocked TNFα induced CXCL8 production (**Figure 6B**). Airway epithelial cells produce basal levels of CXCL8 as demonstrated by the media only controls where there was low, but detectable concentrations of CXCL8. Melanin ghosts suppressed basal levels of CXCL8 production by H292 cells. Inhibition of

transcription by treatment with actinomycin D, did not alter melanin ghosts-induced suppression of basal CXCL8 (**Figure 6B**). Together, these data revealed that the mechanism via which melanin inhibited CXCL8 production was independent of phagocytosis and *de novo* gene transcription.

Melanin exerts a post-translational blockade on CXCL8 secretion

To understand further how melanin acted at a cellular level, we sought to illuminate the mechanism by which melanin interfered with CXCL8 production by epithelial cells. Therefore, we performed paired experiments, in which we stimulated both primary hAEC cultures (**Figure S3A-B**) or H292 monolayers (**Figure 6C-D**) with media alone, wildtype *A. fumigatus* conidia, *ΔpksP* conidia alone or in combination with melanin ghosts, *P. aeruginosa* alone or in combination with melanin ghosts, and melanin ghosts alone. CXCL8 transcription was induced by all stimuli compared with media treatment alone and no significant difference in transcript levels between our pro-inflammatory stimuli (*ΔpksP* or *P. aeruginosa)* either alone or in combination with melanin, demonstrating that melanin ghosts did not block transcription of CXCL8 (**Figure 6D and S3B**). Immunoblotting of epithelial cell lysates revealed increased intracellular CXCL8 in cells treated with melanin ghosts in combination with a pro-inflammatory stimulant (*i.e., ΔpksP* conidia or *P. aeruginosa*) compared to cells treated with the pro-inflammatory stimulant alone (**Figure 6C and S3A**). Interestingly, we observed an increase of intracellular CXCL8 protein within cells treated with melanin ghosts, which is in direct contrast to the decrease in extracellular release of CXCL8 demonstrated by ELISA. These data demonstrated that the difference in extracellular CXCL8 protein in epithelial supernatants was not due to difference in either transcription or translation of the CXCL8 protein. Taken together our results revealed the mechanism of action of melanin on airway epithelial cells. Specifically, melanin interfered with CXCL8 production by airway epithelium through a post-translational blockade of chemokine secretion.

Discussion

Humans are exposed to most fungal pathogens, including *A. fumigatus*, through inhalation of fungal particles including conidia, yeasts, or hyphal fragments. Upon inhalation *Aspergillus* conidia are deposited throughout the host airways, however we lack a fundamental understanding of the role that respiratory epithelium plays in directing the outcome of host-pathogen interaction towards clearance, invasion, or allergic disease. Here, we utilized primary, well differentiated hAEC at ALI and the monomorphic H292 cell line to demonstrate that fungal melanin actively downregulates airway epithelial-driven chemokine responses. Our results demonstrate that *Aspergillus* melanin potently blocks epithelial-driven chemokines via a post-translational inhibition of secretion resulting in the ablation of the chemokine gradient that silences neutrophil transmigration.

The primary hAEC model is powerful model as it recapitulates the pseudostratified structure and cellular diversity of conducting airway epithelium, enabling study of rare populations and the interplay of epithelial cells in disease[24]. Most epithelial cell types cannot be grown in pure cultures, limiting our understanding of the role of specific epithelial cell subtypes in the pathogenesis of disease. While this system has clear advantages over oncogenic and immortalized cell lines, we also confirmed our phenotype in the the cell line, H292, a mucoepitheliod non-small cell lung carcinoma cell line, as this reagent has previously been used extensively in modeling airway epithelial responses to bacterial pathogens[25,34,35,58-60]. While this cell line does not capture the cellular diversity of the airway epithelium, it is well-suited to mechanistic studies due to uniformity of cellular responses and ability to grow large-scale cultures without a dependence on patient sample quality. Importantly, our results demonstrate that melanin effects both pHAEC and H292 epithelial similarly, indicating that H292 cells can serve as a relevant model system for mechanistic dissection of melanin sensing and response pathways.

Prior studies identified an impact on the innate immune sensing of fungal pathogens by fungal melanin. Melanin reprogramed the metabolome of macrophages and prevented LC3-associated phagocytosis of *Aspergillus* conidia through sequestration of calcium preventing calcineurin activation[19,32,61,62]. Additionally, melanin is a known inhibitor of ROS production by phagocytes[12-17], which is an important mechanism of pathogen killing by macrophages and neutrophils. Since the airways are the first point of contact in invasive aspergillosis, we sought to determine the biological role melanin played in innate immune responses. Here, we depict a critical role for fungal melanin in decreasing airway epithelial pro-inflammatory chemokine production via a post-translational mechanism, independent of both phagocytosis or *de novo* transcription. The mechanisms responsible for recognition of fungal melanin by epithelial cells and the post-translational pathway contributing to dampened chemokine secretion remains unknown and warrants further studies. MelLec (also known as Clec1A) is a CLR that recognizes *Aspergillus* DHN melanin, but not L-DOPA melanin of *C. neoformans*[52,61]*.* Both *A. fumigatus* DHN melanin and *C. neoformans* L-DOPA melanin block airway epithelial-derived inflammation suggesting a universal melanin effect at the epithelial surface. Given the specificity of MelLec for only DHN melanin, and the expression of human MelLec is restricted to endothelial cells and innate cells[52], the respiratory epithelial response to melanin is likely independent of MelLec. Our experiments suggest that the phagocytosis of melanin particles is not rnecessary, since cytochalasin D does not block the ability of melanin ghosts to suppress epithelial CXCL8 production, suggesting that melanin is interacting with a cell surface receptor or a soluble factor released by epithelial cells. The observations that multiple forms of melanin retain the capacity to blunt the chemokine secretion by airway epithelial cells suggests that human pathogens exploit this pathway to establish successful infection. Indeed, multiple organisms possess melanin including *A. fumigatus, C. neoformans, Bordatella pertussis,* and *Schistosoma mansoni*[63]*.* Our understanding of melanin is evolving from a structural scaffold that provides protection from the harsh environment it inhabits to a multi-purpose molecules that disables the immune response at multiple steps. Our finding that *Aspergillus* melanin inhibits *P. aeruginosa*-induced airway epithelial chemokine secretion indicates that *Aspergillus* could play a role in

dampening inflammation during co-infections common in CF patients. Colonization by *Aspergillus* could enhance the virulence of *P. aeruginosa* in patients by blocking early innate immune cell recruitment to sites of *P. aeruginosa* infection.

While we focused primarily on CXCL8 for this work, fungal melanin also inhibited the production of CXCL1 (**Figure 2B, S1A, and S2**). While CXCL8 and CXCL1 are known neutrophil chemoattractants that plays a role in epithelial-induced neutrophil transmigration other secreted compounds are also required for *P. aeruginosa* dependent neutrophil transmigration including hepoxilin A3[39-42]. Melanin ghosts dampened neutrophil transmigration in response to *P.aeruginosa,* indicating that the effect of fungal melanin may have a broad impact on airway epithelial cell secretion. Both CXCL8 and CXCL1 are secreted through the trans-Golgi network. The intracellular accumulation of CXCL8 protein with little detectable extracellular CXCL8 suggests that melanin may interfere with trans-Golgi secretion of CXCL8. Future studies will interrogate both traditional trans-Golgi secretomal pathways, as well as alternative secretion systems, such as IL-1β which is secreted via a gasdermin dependent mechanism, to determine the extent of the melanin secretional blockade.

Fungal melanins act as an anti-inflammatory agent at the respiratory epithelium, blocking post-translational secretion of chemokines to recruit host immune cells. *Aspergillus* melanin is required to establish invasive disease as the *ΔpksP* is avirulent in animal models of infection. The mechanism underpinning the virulence defect of the *ΔpksP* strain has long been attributed to melanin blockade of phagosomal maturation and ROS production by innate immune cells, critical requirements for host response to *Aspergillus*. However, our work highlights an additional role for melanin in the host-pathogen interaction, as an anti-inflammatory that prevents airway epithelial chemokine secretion thereby decreasing early recruitment of neutrophils to sites of infection. While there is a clear benefit to the pathogen in preventing inflammatory cell recruitment to the airways, there is potential benefit to the host in dampening host response to melanin at the airway epithelium. If melanin fails to silence inflammation in some patients this could lead to chronic inflammatory

conditions including chronic pulmonary aspergillosis and allergic diseases such as allergic bronchopulmonary aspergillosis and fungal asthma.

Acknowledgements

We would like to thank Drs. Bryan Hurley and Hongmei Mou for insightful discussions regarding our work. Additionally, we would like to thank Dr. George Chamilos for providing melanin ghosts to test in parallel with those created in our own lab. J.L.R is supported by NIH/NIAID grant 1K08AI14755. J.M.V is supported by R01AI150181, R01AI136529, and R21AI152499.

Author Contributions

Conceptualization – Jennifer Reedy and Jatin Vyas. *Investigation* – Jennifer Reedy, Arianne Crossen, Chris Reardon, Hannah Brown Harding. *Writing* – Jennifer Reedy, Rebecca Ward, Arianne Crossen, Jatin Vyas. *Manuscript review and revision* – Arianne Crossen, Hannah Brown Harding, Chris Reardon, Kyle Basham, Rebecca Ward, *Resources* – Jennifer Reedy, Jayaraj Rajagopal and Jatin Vyas.

Declaration of Interest: The authors declare no competing interests.

Figure Legends:

Figure 1. *Aspergillus* melanin inhibits transepithelial migration of neutrophils. (A-B) Neutrophil migration across primary human airway epithelial cells (hAECs) (A) or H292 cells (B) measured by MPO assay following infection (2h hAECs; 1h H292) with 1 x 10^7/cm^2 wildtype B5233 or *ΔpksP A. fumigatus* conidia in the presence or absence of purified *A. fumigatus* melanin ghosts (MG; 5 x 10^7/cm^2). Negative control of media (HBSS) or MG alone were

included. Data represents the number of neutrophils as determined by standard curve. Data are represented as mean ± SEM. n=4-6; One-Way ANOVA with Tukey's multiple comparisons test; **p<0.01, ***p<0.001, ****p<0.0001.

Figure 2. *Aspergillus* melanin inhibits airway epithelial-derived CXCL8 and CXCL1. CXCL8 and CXCL1 in cell supernatants measured by Luminex (A-B) and ELISA (C-F). (A-B) Primary hAECs following 4h stimulation by media alone (HBSS), *P. aeruginosa* PAO1 strain (PSA), three different wildtype (WT) *A. fumigatus* strains (1 x 10^7/cm^2) or *ΔpksP A. fumigatus* conidia (1 x 10^7/cm^2). n=3. (C-D) H292 cells were stimulated for 4h with HBSS, two WT *A. fumigatus* strains, *ΔpksP* conidia, or *ΔpksP* complemented strain (1 x 10^7/cm^2). n=4. (E-F) H292 were stimulated for 4h with HBSS, WT B5233 conidia (1x10^7/cm^2), *ΔpksP* conidia (1x10^7/cm^2), *ΔpksP* conidia mixed with increasing concentrations of *Aspergillus* melanin ghosts (MG; 0.1x = 1x10^6/cm^2; 1x = 1x10^7/cm^2; 10x = 1x10^8/cm^2), or MG alone (1x10^8/cm^2). n=3. Data are represented as mean ± SEM. One-Way ANOVA with Tukey's multiple comparisons test; *p<0.05, **p<0.01, ***p<0.001 compared to *ΔpksP* alone.

Figure 3. The inhibitory effects of *Aspergillus* melanin extended to other pro-inflammatory stimuli. (A) H292 epithelium infected with media alone (HBSS; negative control), *P. aeruginosa* PAO1 strain (PSA) in the absence and presence of increasing *A. fumigatus* melanin ghosts (MG; 0.2x= 2x10^6/cm^2; 1x= 1x10^7/cm^2; 5x= 5x10^7/cm^2) or MG alone for 6h. CXCL8 secretion in the supernatant was measured by ELISA. n=3. See also Figure S1. (B) CXCL8 secretion was measured by ELISA following a 6h stimulation of H292 cells with HBSS, PSA ± MG, TNFα (100 ng/mL) ± MG, or *Aspergillus* MG alone (5x10^7/cm^2). n=3. (C) Neutrophil migration across H292 epithelium in response to PSA alone or in the presence of MG or MG alone (5x10^7/cm^2) was measured by MPO assay. Data represents the number of neutrophils as determined by the standard curve. n=6. (D) 6-12-week-old C57BL/6 mice were infected via

oropharyngeal aspiration with PSA ($5.85x10^5$) with or without *Aspergillus* MG ($5.85x10^6$) for 4h. The number of neutrophils in the bronchoalveolar lavage fluid was measured by flow cytometry. n=2-3. Data are represented as mean ± SEM. One-Way ANOVA with Tukey's multiple comparisons test; *p<0.05, **p<0.01, ***p<0.001, ****p<0.0001 compared to stimulation alone (*i.e.,* PSA or TNFα alone).

Figure 4. *Structurally distinct melanins from diverse sources block airway epithelial CXCL8.* (A) H292 cells were stimulated for 6h with wildtype *A. fumigatus* (B5233; $1x10^7/cm^2$), *ΔpksP* conidia ($1x10^7/cm^2$) with or without *C. neoformans* H99 melanin ghosts (*Cn*-MG) ($5x10^7/cm^2$), *P. aeruginosa* PAO1 strain (PSA) with or without *Cn*-MG, or *Cn*-MG alone. CXCL8 secretion was measured by ELISA. See also Figure S2. (B) H292 epithelium was infected with PSA in the absence or presence of synthetic L-DOPA-coated FLP ($5x10^7/cm^2$), β-1,3-glucan-coated FLP (BG; $5x10^7/cm^2$), or naked FLP ($5x10^7/cm^2$) for 6h, then CXCL8 was measured by ELISA. Media or coated beads alone were included as negative controls. Data are represented as mean ± SEM. n=3; Unpaired t-test; *p<0.05, **p<0.01, ****p<0.0001 compared to stimulation alone (*i.e., ΔpksP* or PSA alone).

Figure 5. Melanin abolished the transepithelial gradient of CXCL8 required for neutrophil transmigration, with a durable impact on CXCL8 secretion. (A) CXCL8 expression in the media from the apical (A) and basolateral (BL) sides of H292 cells was measured by ELISA. H292 cells were infected for 6h with *P. aeruginosa* PAO1 strain (PSA) and *Aspergillus* melanin ghosts (MG; $5x10^7/cm^2$) together or alone. Media alone (HBSS) was used as a negative control. n=6; one-way ANOVA with Tukey's multiple comparisons test. (B) An ELISA assessed CXCL8 levels following a 24h stimulation with PSA or TNFα (100 ng/mL) in the absence or presence of MG ($5x10^7/cm^2$). n=3; two-way ANOVA with Sidak's multiple comparison test. Data are represented as mean ± SEM. ***p<0.001, ****p<0.0001.

Figure 6. Melanin suppression of chemokine production is independent of phagocytosis of melanin or *de novo* transcription, but exerts a post-translational blockade on CXCL8 secretion. (A) H292 cells were incubated with DMSO vehicle control or cytochalasin D (CytoD; 20µM) for 30 min, then stimulated with TNFα (100 ng/mL) and/or *Aspergillus* melanin ghosts (MG; $2x10^7/cm^2$) for 6h. Apical CXCL8 levels were measured by ELISA. n=3 (B) H292 epithelium was exposed to Actinomycin D (1µg/mL), then stimulated as described in A. CXCL8 secretion was measured using an ELISA assay. n=3. (C-D) CXCL8 expression in H292 cells lysates was measured by (C) qPCR for RNA and (D) Western blot for intracellular protein, respectively, following 6h stimulation with *A. fumigatus* wildtype (WT; B5233 strain; $1x10^7/cm^2$), *ΔpksP* conidia ($1x10^7/cm^2$) ± MG, *P. aeruginosa* PAO1 strain (PSA) ± MG, or MG alone ($5x10^7/cm^2$). For Western blots, GAPDH was used as a loading control. See also Figure S3. n=2. Data are represented as mean ± SEM. Unpaired t-test; **p<0.01; ****p<0.0001.

Materials and Methods:

H292 culture, upright and inverted Transwell culture

Human NCI-H292 pulmonary mucoepidermoid carcinoma cell line (H292) (American Type Cell Collection) was grown as previously described[26,42,58,59]. H292 cells were cultured in complete RPMI medium (cRMPI) (RPMI 1640, L-glutamine, 10% heat-inactivated fetal bovine serum [FBS] (Gibco) and 1% penicillin/streptomycin) at 37°C in the presence of 5% CO2. For upright Transwell culture, the apical compartments of Costar 6.5 mm or 12mm Transwell® inserts with 0.4 µm pore polyester membrane were treated with a 60% Ethanol, 1:100 rat tail collagen I (Corning) mixture and left open in tissue culture hood for at least 4h to allow for evaporation. H292 cells were then liberated with 0.25% Trypsin-EDTA **(**Thermo Fisher Scientific) and resuspended in cRPMI. The cell suspension was seeded onto the apical surface of the

Transwells and cRPMI was added to the basolateral compartment. For inverted Transwell culture for use in neutrophil migration assays, Costar 6.5 mm Transwell® inserts with 3.0 µm pore polyester membranes (Corning) were inverted and treated with collagen. H292 cells in suspension were applied to the surface of the inverted Transwells to form a small tension bubble and incubated overnight. The following day, Transwells were placed upright in a Costar culture plate (Corning) and both the apical and basolateral compartments were filled with cRPMI. All transwell cultures were incubated at 37°C in the presence of 5% CO_2 and used on day 7.

Primary human airway epithelial basal cell proliferation and upright and inverted ALI Transwell Culture

Primary hAEC were grown as previously described[26,35,64-66]. Basal cells were cultured in small-airway epithelial cell medium (SAGM) (PromoCell) supplemented with 5 µM Y-27632, 1 µM A-83-01, 0.2 µM DMH-1, and 0.5 µM CHIR99021 and 1% penicillin/streptomycin on laminin-enriched 804G-conditioned media coated plates. For differentiation of basal cells into a fully pseudostratified epithelium at ALI, the apical compartments of Costar 6.5 mm or 12mm Transwell® inserts with 0.4 µm pore polyester membrane were coated with 804G-conditioned media for at least 4 hours. Upon removal, a basal cell suspension in SAGM was applied to the apical compartment, and SAGM was added to the basolateral compartment and the transwells were incubated overnight. The following day, the SAGM was replaced with PneumaCult-ALI medium combined 1:1 with Gibco DMEM/F-12 and incubated overnight. The media in the apical compartment was then removed to establish ALI. ALI hAEC were incubated for 16-21 days wherein the apical compartment is kept dry and the ALI media in the basolateral compartment is refreshed frequently.

For inverted ALI culture for use in neutrophil migration assays, Costar 6.5 mm Transwell® inserts with 3.0 µm pore polyester membranes (Corning) were inverted and treated

with 804G-conditioned media. Basal cells in suspension in SAGM were applied to the surface of the inverted Transwells to form a small tension bubble and incubated overnight. The following day, Transwells were placed upright in a Costar culture plate (Corning) and both the apical and basolateral compartments were filled with SAGM. The following day, SAGM was replaced with PneumaCult-ALI medium combined 1:1 with Gibco DMEM/F-12 and incubated overnight. The media in the apical compartment was then removed to establish air-liquid interface. The inverted ALI were incubated for 16-21 days wherein the apical compartment is kept dry and the media in the basolateral compartment is refreshed frequently. All ALI cultures were incubated at 37°C in the presence of 5% CO_2. Prior to use, the transepithelial electrical resistance (TEER) was measured on the day of experiment to ensure that all epithelium were intact.

Fungal and bacterial Culture

Aspergillus fumigatus strains Af293, CEA10, B5233, ΔpksP, and *ΔpksP* + pksP were used. The *B5233, ΔpksP,* and complemented *ΔpksP* + pksP strains were gifted by K.J. Kwon-Chung (National Institutes of Health; NIH). All *A. fumigatus* strains were grown at 37°C for 3 – 5 days on glucose minimal media slants (GMM). Conidia were harvested by applying a sterile solution of deionized water (Milli-Q, Millipore Sigma, Burlington, MA) containing 0.01% Tween 20 to each slant followed by gentle surface agitation to liberate conidia using a sterile cotton-tipped swab. The solution was passed through a 40 μm cell strainer to separate conidia from hyphal fragments. Conidia were then washed three times with sterile PBS and counted on a LUNA™ automated cell counter (Logos Biosystems). Conidia were used either on the day of harvest or stored at 4°C overnight for use the following day. For animal experiments, conidia were used on the day of harvest.

P. aeruginosa strain PAO1 was grown overnight in 4 mL of LB liquid media at 37°C with shaking. Cultures were inoculated from frozen stocks of PAO1 stored at -80°C. After shaking

overnight, 1 mL of overnight culture was centrifuged at 16,000 g x 5 minutes and washed three times in HBSS. After the final wash the *P. aeruginosa* was resuspended in 600 μl of HBSS. For *in vitro* stimulations, the *P. aeruginosa* was used at a 1:100 dilution. For quantification of bacterial number for *in vivo* experiments, the OD600 of a 1:10 dilution of bacteria in HBSS was obtained and bacteria were diluted appropriately.

Neutrophil isolation

Neutrophils were isolated from healthy volunteer donors in accordance with Massachusetts General Hospital IRB-approved protocol (2015P000818) as previously described[26,59]. Briefly, 50 mL of blood was drawn via venipuncture into a syringe containing acid citrate-dextrose. The blood was split between three 50 mL conical tubes and layered on top of a Ficoll-Paque solution, then centrifuged at 2200 rpm for 20 minutes at room temperature to obtain a buffy coat layer. Plasma and mononuclear cells were removed by aspiration. Red blood cells (RBC) were removed using 2% gelatin sedimentation technique followed by a wash with RBC lysis buffer. The remaining neutrophils were washed and resuspended in HBSS without calcium or magnesium (HBSS-) to a concentration of 5×10^7 neutrophils/mL.

Neutrophil transmigration experiments

The neutrophil transepithelial migration experiments were performed as previously described[26,35,36,59]. H292 cell monolayers or primary hAEC were grown on the underside of 3.0 μm pore size Transwell filters (Corning Life Sciences) to enable neutrophil migration through the Transwell. Mature epithelium (at least 16 days at ALI for primary hAECs or day 7 monolayers of H292 cells) in 12 well format were used for all experiments. On the day of the experiment, Transwells were equilibrated in HBSS for at least 30 minutes prior to stimulation. Transwells were then inverted into a sterile 15 cm cell culture plate and infected on the apical surface.

Cells were stimulated with media only (HBSS), *P. aeruginosa* (PAO1), *A. fumigatus* conidia, or melanin ghosts. Infections were for 1 h on H292 cell monolayers and for 2 h on primary hAEC. After stimulation, the apical surface was washed and transwells were inverted into fresh 24 well culture plates containing HBSS alone or HBSS containing 100 nM *N*-formyl-methionyl-leucyl-phenylalanine (fMLP; Sigma; uninfected positive control). Neutrophils were applied to the basolateral compartment and transmigration was allowed to proceed for 2h (H292 cells) and 4h (primary hAECs) at 37°C with 5% CO_2. After the migration period, the Transwells were discarded and the migrated neutrophils were quantified using a myeloperoxidase (MPO) assay. The migrated neutrophils in the apical compartment were lysed with 0.5% Triton X-100 and neutrophil MPO activity was quantified using a colorimetric assay using citrate buffered 2,2'-azino-bis(3-ethylbenxothiazoline-6-sulfonic acid) diammonium salt (ABTS) solution. After 10 min of incubation, the optical density at 405 nm was read using a spectrophotometer plate reader. In addition, to the experimental samples, a standard curve was prepared for each experiment was used to determine the number of migrated neutrophils based on the OD_{405} value. Data are displayed as the number of transmigrated neutrophils, extrapolated from the standard curve.

Melanin ghost preparation

Melanin ghosts were prepared using previously published methods[18,29-33]. In addition to melanin ghosts created in our lab using the following protocol, we also tested melanin ghosts created in the laboratory of Dr. George Chamilos with similar results to our own. Briefly, *A. fumigatus* strain B5233 was grown for 3 days in T75 flasks (CELLTREAT) on GMM at 30°C. Flasks were seeded from frozen stocks of conidia maintained at −80°C. To harvest conidia, a sterile solution of deionized water (Milli-Q; Millipore Sigma) containing 0.01% Tween 20 (Sigma-Aldrich) was added to each flask, and spores were liberated using gentle surface agitation with a sterile swab. The spore solution was passed through a 40-μm cell strainer to separate hyphal debris.

To remove the fungal cell wall, spores were washed three times with sterile PBS, then resuspended in 10mg/mL lysing enzymes from *Trichoderma harzianum* which has since been discontinued and replaced with 5mg/mL lyticase from *Arthrobacter luteus* (Sigma-Aldrich) dissolved in a 1 M Sorbitol (Sigma-Aldrich) / 0.1 M Sodium Citrate (Sigma-Aldrich) solution in deionized water. The solution was incubated in a 30°C water bath for 24h. To denature proteins, the spore solution was then washed twice with sterile PBS and resuspended in a 4 M guanidine thiocyanate (Sigma-Aldrich) solution and incubated at room temperature for 18h with nutation. To hydrolyze proteins, spores were then washed twice with sterile PBS and resuspended in a 1.0 mg/mL Proteinase K (Roche Laboratories) in 10mM Tris-HCl (Sigma-Aldrich), 1mM $CaCl_2$ (Sigma-Aldrich), and 0.5% Sodium Dodecyl Sulfate (Sigma-Aldrich) pH 7.8, solution in distilled water. The suspension was incubated in a 65°C water bath for 4h, then washed three times with sterile PBS and resuspended in a 0.9% NaCl solution. A Folch lipid extraction was then performed wherein the suspension was transferred to a separatory funnel along with methanol (Thermo Fisher Scientific) and chloroform (Midland Scientific) and mixed vigorously. This was repeated twice, with the organic layer being drained each time and the soluble melanin-containing interfacial layer maintained. For the hydrolysis of residual acid-labile constituents, 6M HCl (Thermo Fisher Scientific) was added to the flask and boiled for 1 hour, then combined with equal volume sterile PBS to neutralize pH. The melanin ghost suspension was then washed with sterile PBS and placed in 0.22 µm centrifugal filter units (Merck Millipore Ltd). The melanin ghosts were then washed 3 times and resuspended in deionized water. The suspension was frozen overnight at -80°C and lyophilized for two days. The melanin ghosts were finally resuspended in sterile PBS, sonicated, and counted on a LUNA automated cell counter (Logos Biosystems).

Fungal-like particle (FLP) creation

We have previously created FLP using purified fungal carbohydrates which we can associated

with amine-coated polystyrene 3 μM microspheres using either chemical conjugation or adsorption[53,54]. To create melanin-coated particles, synthetic melanin (Sigma) was sonicated robustly in DMSO to create a fine suspension that was then incubated with amine-coated polystyrene microspheres for 1h at room temperature with shaking. The microspheres were washed copiously with PBS to remove all traces of DMSO and free melanin particles. All of the microspheres obtained a brown coloration consistent with melanin association and there was no free melanin visible in the flow through from the FLP.

ELISA

Mature epithelium (at least 16 days at ALI for primary hAECs or day 7 monolayers of H292 cells) in either 12 or 24 well format were used for all experiments. On the day of the experiment, growth media was removed and cells were equilibrated for at least 30 min in HBSS. HBSS was removed and replaced with fresh HBSS alone or containing the appropriate stimulants. Since the primary hAEC are pseudostratified epithelium, the concentration of applied stimuli was based upon the surface area of the epithelium rather than an MOI calculation. After application of stimuli, cell culture plates were spun gently at 1000 rpm x 5 min to bring pathogens in contact with epithelial surface. Stimulations were allowed to proceed for the desired time (4h – 24h). Supernatants were harvest and centrifuged through Captiva 96 well 0.2 uM filter plate at 3000 rpm for 10 min. Supernatants were frozen at -80°C until use. ELISAs were performed using either R&D Duoset kits or Biolegend LegendPlex assays according to the manufacturers instructions. For the R&D Duoset kits the ELISA were read using an i3X Spectrophotometer (Molecular Devices, LLC). For the LegendPlex assays, a BD FACSCelesta™ Flow Cytometer (BD) was used for data acquisition. The resultant flow cytometry files were then analyzed using the LEGENDplex™ Data Analysis Software Suite. Results were analyzed using GraphPad

PRISM9 software (GraphPad Software). All reported ELISAs were done in both technical and biological triplicate.

For cytochalasin D experiments, cytochalasin D was added to HBSS media at a final concentration of 20 μM. Epithelial cells were incubated for 30 min at 37°C prior to stimulation. At that time the media was exchanged for fresh HBSS containing the indicated stimulants in addition to 20 μM cytochalasin D. To inhibit transcription, actinomycin D dissolved in DMSO was added to HBSS at a final concentration of 1μg/mL. An equal volume of DMSO in HBSS was added to the control wells. Epithelial cells were then incubated for 1h at 37°C prior to stimulation.

***In vivo* neutrophil recruitment experiment**

C57BL/6 mice of 6 -12 weeks of age were obtained from Jackson Laboratories and housed in the Massachusetts General Hospital specific pathogen-free animal facilities for at least one week prior to infection. *Pseudomonas* strain PAO1 was diluted and quantified using OD600. Inoculums were prepared consisting of HBSS alone, 5.8 x 10^5 CFU PaO1 alone, 5.9 x 10^6 melanin ghosts alone, or a 5.8 x 10^5 CFU PAO1 combined with 5.8 x 10^6 melanin ghosts. Each inoculum was prepared in 50 μl total volume in HBSS. Mice were infected via oropharyngeal aspiration of the inoculum under isoflurane anesthesia. Infection was allowed to proceed for 4 hours, at which time mice were euthanized using CO_2. Mice were exsanguinated, and the trachea was exposed and cannulated with a 22G catheter (Exel Safelet Catheter) that was secured in place using suture string. The lungs were flushed with a total of 2.3 ml of PBS containing 5% fetal bovine serum. The collected bronchoalveolar lavage fluid was centrifuged at 300 g x 5 min to pellet cells. The pelleted cells were resuspended in FACS buffer (PBS + 2% bovine serum albumin) containing 1:100 dilution of Fc Block and a 1:250 dilution of Zombie Violet dye. After incubation at 4^{0}C for 15 minutes, cells were centrifuged and then resuspended

in FACS buffer containing an antibody cocktail consistent of anti-CD11b APCFire, anti-CD45 BV605, and anti- Ly6G AF488. After incubation at 4°C for 20 min cells were washed with FACS buffer and then fixed in 4% paraformaldehyde for 10 min at room temperature. Cells were washed and then resuspended in FACs buffer and stored at 4°C (cells were stored no longer than overnight prior to flow cytometry). Splenocytes for a single mouse were prepared in parallel to use as controls for flow cytometry gating. Counting beads were added prior to flow and calibration beads were prepared using each of the fluorophores. Samples were run on a a BD FACSCelesta™ Flow Cytometer, and analysis was performed using FlowJo 10 software (BD). Three mice were used per experimental group. All animal studies were conducted under protocols approved by the Institutional Animal Care and Use Committee Subcommittee on Research Animal Care at Massachusetts General Hospital.

RNA extraction and qRT-PCR

Epithelium was grown on 0.4 µm pore-size Transwells until mature (at least 16 days hAEC or 7 days for H292 cells). On the day of stimulation, media was removed and cells were equilibrated in HBSS for at least 30 min prior to stimulation with either media alone (HBSS), *Pseudomonas aeruginosa* (PAO1), *A. fumigatus* conidia or melanin ghosts alone or in combination. Conidia were applied at 1 x 10^7 conidia per cm^2 and melanin ghosts were applied at 5X concentration at 5 x 10^7 conidia per cm^2. After 6h of stimulation, supernatants were harvested for ELISA. At least 4 Transwells of epithelium were stimulated per condition, one well of epithelium was used for Western blot analysis and three wells were each harvested for RNA. For RNA prep, the epithelium was washed with ice-cold HBSS and then RNA was isolated using the QIAGEN RNeasy Mini Kit. After harvest of cell lysates in QIAGEN RLT buffer containing beta-mercaptoethanol, cell lysates were transferred to QIAGEN QIAshredder columns to homogenize the cells, the rest of the RNA extraction was performed according to RNeasy mini kit

instructions. RNA was quantified using nanodrop. cDNA was created using the SuperScript IV VILO kit (Thermo Fisher Scientific) according to manufacturers instructions. qRT-PCR was performed on cDNA using the Taqman® Fast Advanced Master Mix and Taqman® Gene Expression assay probes CXCL8 labelled with FAM and GAPDH labelled with VIC-MGB. qRT-PCR reactions were run using the Applied Biosystems™ 7500 Fast Real-Time PCR System per kit instructions and analyzed using the ΔΔCt method. All qRT-PCR experiments were performed in at least biological duplicates.

Western blot

Epithelium were prepared as described in "RNA extraction and qRT-PCR". After 6h of stimulation the epithelium was placed on ice and lysed with 1% NP40 lysis buffer containing protease inhibitor. Following denaturation with NuPAGE LDS Sample Buffer (Thermo Fisher Scientific) proteins were resolved by SDS-PAGE on NuPAGE gels (NuPAGE gels, Thermo Fisher Scientific). Proteins were then transferred to methanol-activated PDVF membrane (Perkin Elmer) using transfer buffer (0.025M Tris, 0.192 M glycine, 20% methanol) and electrophoretic transfer at 100V for 1h. The membranes were blocked for 1h at room temperature in 5% Milk in PBS-0.01% Tween 20 (PBST), and then incubated with anti-CXCL8 antibody overnight at 4°C. Membranes were washed and incubated for 1h at room temperature with secondary HRP conjugated antibody. After washing, membranes were visualized using Western Lightning Plus ECL chemiluminescent substrate (Perkin Elmer, Waltham, MA) and developed using Kodak BioMax XAR film (Millipore Sigma). Films were then scanned and processed using Adobe Photoshop 2021. Any contrast adjustments were applied evenly to the entire image and adheres to the standards set forth by the scientific community[67]. All reported western blots were repeated in at least biological duplicate.

Luminex assay

24- well Transwells were prepared using basal epithelial cells from three healthy human donors and differentiated for 16 days at ALI. On the day of stimulation, ALI media was removed and epithelium were equilibrated in HBSS media for 1.5h prior to stimulation. The HBSS was removed and replaced with fresh HBSS media on the basolateral side, and 200 μL of HBSS media containing 1 x 10^7/cm^2 wild type conidia (strains CEA10, Af293, B5233), *ΔpksP* conidia or *P. aeruginosa* strain PAO1. After 4h, the apical and basolateral media was harvested and put through a Captiva 96 well 0.2 μm filter plate at 3000 rpm for 10 min. Supernatants were frozen at -80°C. Data were processed using the Luminex analytical software. MILLIPLEX Map Human cytokine/chemokine Magnetic Bead Panel – Premixed 41 Plex, run on a MAGPIX® xMAP instrument according to manufacturer's instructions. Analysis was performed using GraphPad Prism.

Pseudomonas epithelial association assay

H292 epithelium were infected with PAO1 alone or in combination with 5x10^7 *Aspergillus* melanin ghosts and incubated for 4h. Wells were washed three times with HBSS to remove any nonadherent bacteria. To lyse epithelial cells, 1% Triton X-100 was added to each well, and plates were incubated with gentle agitation for 1h at 4°C. The lysate was collected, vortexed, and 1:10 serial dilutions were made in HBSS. 100 μL of each dilution was plated onto LB agar plates containing ampicillin and spread using glass beads. The plates were incubated at 37°C overnight and colony forming units were counted the following day.

LDH viability assay

The LDH viability assay was performed using Invitrogen CyQUANT LDH Cytotoxicity Assay according to the manufacturers instructions. After 6h infection of H292 cells, a 1:10 dilution of 1% Triton X-100 was added to control well containing unstimulated epithelium to lyse the cells

and incubated for 10 min at 37°C 5% CO_2. 50 µL of supernatant from each experimental condition (all experimental conditions were performed in triplicate) was transferred to a 96 well plate and mixed with 50 µL of the kit Reaction mixture and allowed to incubated for 30 min at room temperature in the dark. Stop solution was then added to each sample and absorbance at 490 and 680 was measured using an i3X Spectrophotometer (Molecular Devices, LLC). LDH activity and % cytotoxicity were calculated according to assay kit instructions.

REFERENCES

1. Thompson, G.R., 3rd, and Young, J.H. (2021). *Aspergillus* infections. N Engl J Med *385*, 1496-1509. 10.1056/NEJMra2027424.

2. Huang, L., Zhang, N., Huang, X., Xiong, S., Feng, Y., Zhang, Y., Li, M., and Zhan, Q. (2019). Invasive pulmonary aspergillosis in patients with influenza infection: A retrospective study and review of the literature. Clin Respir J *13*, 202-211. 10.1111/crj.12995.

3. Rawson, T.M., Moore, L.S.P., Zhu, N., Ranganathan, N., Skolimowska, K., Gilchrist, M., Satta, G., Cooke, G., and Holmes, A. (2020). Bacterial and fungal coinfection in individuals with coronavirus: a rapid review to support COVID-19 antimicrobial prescribing. Clin Infect Dis *71*, 2459-2468. 10.1093/cid/ciaa530.

4. Rayens, E., Norris, K.A., and Cordero, J.F. (2021). Mortality trends in risk conditions and invasive mycotic disease in the United States, 1999-2018. Clin Infect Dis *74*, 309-318. 10.1093/cid/ciab336.

5. Takazono, T., and Sheppard, D.C. (2017). *Aspergillus* in chronic lung disease: modeling what goes on in the airways. Med Mycol *55*, 39-47. 10.1093/mmy/myw117.

6. Bueid, A., Howard, S.J., Moore, C.B., Richardson, M.D., Harrison, E., Bowyer, P., and Denning, D.W. (2010). Azole antifungal resistance in *Aspergillus fumigatus*: 2008 and 2009. J Antimicrob Chemother *65*, 2116-2118. 10.1093/jac/dkq279.

7. Iversen, M., Burton, C.M., Vand, S., Skovfoged, L., Carlsen, J., Milman, N., Andersen, C.B., Rasmussen, M., and Tvede, M. (2007). *Aspergillus* infection in lung transplant patients: incidence and prognosis. Eur J Clin Microbiol Infect Dis *26*, 879-886. 10.1007/s10096-007-0376-3.

8. Lin, S.J., Schranz, J., and Teutsch, S.M. (2001). Aspergillosis case-fatality rate: systematic review of the literature. Clin Infect Dis *32*, 358-366. 10.1086/318483.

9. Ward, R.A., and Vyas, J.M. (2020). The first line of defense: effector pathways of anti-fungal innate immunity. Curr Opin Microbiol *58*, 160-165. 10.1016/j.mib.2020.10.003.

10. Latgé, J.P., Beauvais, A., and Chamilos, G. (2017). The Cell Wall of the Human Fungal Pathogen A*spergillus fumigatus*: Biosynthesis, Organization, Immune Response, and Virulence. Annu Rev Microbiol *71*, 99-116. 10.1146/annurev-micro-030117-020406.

11. Valsecchi, I., Dupres, V., Michel, J.P., Duchateau, M., Matondo, M., Chamilos, G., Saveanu, C., Guijarro, J.I., Aimanianda, V., Lafont, F., et al. (2019). The puzzling construction of the conidial outer layer of *Aspergillus fumigatus*. Cell Microbiol *21*, e12994. 10.1111/cmi.12994.

12. Wang, Y., Aisen, P., and Casadevall, A. (1995). *Cryptococcus neoformans* melanin and virulence: mechanism of action. Infect Immun *63*, 3131-3136. 10.1128/iai.63.8.3131-3136.1995.

13. Jahn, B., Koch, A., Schmidt, A., Wanner, G., Gehringer, H., Bhakdi, S., and Brakhage, A.A. (1997). Isolation and characterization of a pigmentless-conidium mutant of *Aspergillus fumigatus* with altered conidial surface and reduced virulence. Infect Immun *65*, 5110-5117. 10.1128/iai.65.12.5110-5117.1997.

14. Langfelder, K., Jahn, B., Gehringer, H., Schmidt, A., Wanner, G., and Brakhage, A.A. (1998). Identification of a polyketide synthase gene (pksP) of *Aspergillus fumigatus* involved in conidial pigment biosynthesis and virulence. Med Microbiol Immunol *187*, 79-89.

15. Tsai, H.F., Chang, Y.C., Washburn, R.G., Wheeler, M.H., and Kwon-Chung, K.J. (1998). The developmentally regulated *alb1* gene of *Aspergillus fumigatus*: its role in modulation of conidial morphology and virulence. J Bacteriol *180*, 3031-3038.

16. Sugareva, V., Hartl, A., Brock, M., Hubner, K., Rohde, M., Heinekamp, T., and Brakhage, A.A. (2006). Characterisation of the laccase-encoding gene abr2 of the dihydroxynaphthalene-like melanin gene cluster of *Aspergillus fumigatus*. Arch Microbiol *186*, 345-355. 10.1007/s00203-006-0144-2.

17. Chai, L.Y., Netea, M.G., Sugui, J., Vonk, A.G., van de Sande, W.W., Warris, A., Kwon-Chung, K.J., and Kullberg, B.J. (2010). *Aspergillus fumigatus* conidial melanin modulates host cytokine response. Immunobiology *215*, 915-920. 10.1016/j.imbio.2009.10.002.

18. Akoumianaki, T., Kyrmizi, I., Valsecchi, I., Gresnigt, M.S., Samonis, G., Drakos, E., Boumpas, D., Muszkieta, L., Prevost, M.C., Kontoyiannis, D.P., et al. (2016). *Aspergillus* cell wall melanin blocks LC3-associated phagocytosis to promote pathogenicity. Cell Host Microbe *19*, 79-90. 10.1016/j.chom.2015.12.002.

19. Goncalves, S.M., Duarte-Oliveira, C., Campos, C.F., Aimanianda, V., Ter Horst, R., Leite, L., Mercier, T., Pereira, P., Fernandez-Garcia, M., Antunes, D., et al. (2020). Phagosomal removal of fungal melanin reprograms macrophage metabolism to promote antifungal immunity. Nat Commun *11*, 2282. 10.1038/s41467-020-16120-z.

20. Kradin, R.L., and Mark, E.J. (2008). The pathology of pulmonary disorders due to *Aspergillus spp*. Arch Pathol Lab Med *132*, 606-614. 10.5858/2008-132-606-TPOPDD.

21. Latge, J.P. (2001). The pathobiology of *Aspergillus fumigatus*. Trends Microbiol *9*, 382-389. 10.1016/s0966-842x(01)02104-7.

22. Lee, J.Y., Joo, E.J., Yeom, J.S., Song, J.U., Yim, S.H., Shin, D.S., Yu, J.H., Ju, D.Y., Yim, J.W., Song, Y.S., et al. (2014). *Aspergillus* Tracheobronchitis and Influenza A Co-infection in a Patient with AIDS and Neutropenia. Infect Chemother *46*, 209-215. 10.3947/ic.2014.46.3.209.

23. Nyga, R., Maizel, J., Nseir, S., Chouaki, T., Milic, I., Roger, P.A., Van Grunderbeeck, N., Lemyze, M., Totet, A., Castelain, S., et al. (2020). Invasive Tracheobronchial Aspergillosis in Critically Ill Patients with Severe Influenza. A Clinical Trial. Am J Respir Crit Care Med *202*, 708-716. 10.1164/rccm.201910-1931OC.

24. Montoro, D.T., Haber, A.L., Biton, M., Vinarsky, V., Lin, B., Birket, S.E., Yuan, F., Chen, S., Leung, H.M., Villoria, J., et al. (2018). A revised airway epithelial hierarchy includes CFTR-expressing ionocytes. Nature *560*, 319-324. 10.1038/s41586-018-0393-7.

25. Yonker, L.M., Pazos, M.A., Lanter, B.B., Mou, H., Chu, K.K., Eaton, A.D., Bonventre, J.V., Tearney, G.J., Rajagopal, J., and Hurley, B.P. (2017). Neutrophil-Derived Cytosolic PLA2α Contributes to Bacterial-Induced Neutrophil Transepithelial Migration. J Immunol *199*, 2873-2884. 10.4049/jimmunol.1700539.

26. Feldman, M.B., Dutko, R.A., Wood, M.A., Ward, R.A., Leung, H.M., Snow, R.F., De La Flor, D.J., Yonker, L.M., Reedy, J.L., Tearney, G.J., et al. (2020). *Aspergillus fumigatus* Cell Wall Promotes Apical Airway Epithelial Recruitment of Human Neutrophils. Infect Immun *88*. 10.1128/IAI.00813-19.

27. Feldman, M.B., Wood, M., Lapey, A., and Mou, H. (2019). SMAD Signaling Restricts Mucous Cell Differentiation in Human Airway Epithelium. Am J Respir Cell Mol Biol *61*, 322-331. 10.1165/rcmb.2018-0326OC.

28. Yonker, L.M., Marand, A., Muldur, S., Hopke, A., Leung, H.M., De La Flor, D., Park, G., Pinsky, H., Guthrie, L.B., Tearney, G.J., et al. (2021). Neutrophil dysfunction in cystic fibrosis. J Cyst Fibros *20*, 1062-1071. 10.1016/j.jcf.2021.01.012.

29. Wang, Y., Aisen, P., and Casadevall, A. (1996). Melanin, melanin "ghosts," and melanin composition in *Cryptococcus neoformans*. Infect Immun *64*, 2420-2424. 10.1128/iai.64.7.2420-2424.1996.

30. Rosas, A.L., Nosanchuk, J.D., Feldmesser, M., Cox, G.M., McDade, H.C., and Casadevall, A. (2000). Synthesis of polymerized melanin by *Cryptococcus neoformans* in infected rodents. Infect Immun *68*, 2845-2853. 10.1128/IAI.68.5.2845-2853.2000.

31. Folch, J., Lees, M., and Sloane Stanley, G.H. (1957). A simple method for the isolation and purification of total lipides from animal tissues. J Biol Chem *226*, 497-509.

32. Chamilos, G., Akoumianaki, T., Kyrmizi, I., Brakhage, A., Beauvais, A., and Latge, J.P. (2016). Melanin targets LC3-associated phagocytosis (LAP): A novel pathogenetic mechanism in fungal disease. Autophagy *12*, 888-889. 10.1080/15548627.2016.1157242.

33. Camacho, E., Chrissian, C., Cordero, R.J.B., Liporagi-Lopes, L., Stark, R.E., and Casadevall, A. (2017). N-acetylglucosamine affects *Cryptococcus neoformans* cell-wall composition and melanin architecture. Microbiology (Reading) *163*, 1540-1556. 10.1099/mic.0.000552.

34. Pazos, M.A., Lanter, B.B., Yonker, L.M., Eaton, A.D., Pirzai, W., Gronert, K., Bonventre, J.V., and Hurley, B.P. (2017). *Pseudomonas aeruginosa* ExoU augments neutrophil transepithelial migration. PLoS Pathog *13*, e1006548. 10.1371/journal.ppat.1006548.

35. Yonker, L.M., Mou, H., Chu, K.K., Pazos, M.A., Leung, H., Cui, D., Ryu, J., Hibbler, R.M., Eaton, A.D., Ford, T.N., et al. (2017). Development of a Primary Human Co-Culture Model of Inflamed Airway Mucosa. Sci Rep *7*, 8182. 10.1038/s41598-017-08567-w.

36. Yonker, L.M., Pazos, M.A., Lanter, B.B., Mou, H., Chu, K.K., Eaton, A.D., Bonventre, J.V., Tearney, G.J., Rajagopal, J., and Hurley, B.P. (2017). Neutrophil-Derived Cytosolic PLA2alpha Contributes to Bacterial-Induced Neutrophil Transepithelial Migration. J Immunol *199*, 2873-2884. 10.4049/jimmunol.1700539.

37. Das, S.T., Rajagopalan, L., Guerrero-Plata, A., Sai, J., Richmond, A., Garofalo, R.P., and Rajarathnam, K. (2010). Monomeric and dimeric CXCL8 are both essential for *in vivo* neutrophil recruitment. PLoS One *5*, e11754. 10.1371/journal.pone.0011754.

38. Long, M.B., and Chalmers, J.D. (2022). Treating Neutrophilic Inflammation in Airways Diseases. Arch Bronconeumol *58*, 463-465. 10.1016/j.arbres.2021.11.003.

39. Tamang, D.L., Pirzai, W., Priebe, G.P., Traficante, D.C., Pier, G.B., Falck, J.R., Morisseau, C., Hammock, B.D., McCormick, B.A., Gronert, K., and Hurley, B.P. (2012). Hepoxilin A(3) facilitates neutrophilic breach of lipoxygenase-expressing airway epithelial barriers. J Immunol *189*, 4960-4969. 10.4049/jimmunol.1201922.

40. Pazos, M.A., Pirzai, W., Yonker, L.M., Morisseau, C., Gronert, K., and Hurley, B.P. (2015). Distinct cellular sources of hepoxilin A3 and leukotriene B4 are used to coordinate bacterial-induced neutrophil transepithelial migration. J Immunol *194*, 1304-1315. 10.4049/jimmunol.1402489.

41. Mrsny, R.J., Gewirtz, A.T., Siccardi, D., Savidge, T., Hurley, B.P., Madara, J.L., and McCormick, B.A. (2004). Identification of hepoxilin A3 in inflammatory events: a required role in neutrophil migration across intestinal epithelia. Proc Natl Acad Sci U S A *101*, 7421-7426. 10.1073/pnas.0400832101.

42. Kubala, S.A., Patil, S.U., Shreffler, W.G., and Hurley, B.P. (2014). Pathogen induced chemo-attractant hepoxilin A3 drives neutrophils, but not eosinophils across epithelial barriers. Prostaglandins Other Lipid Mediat *108*, 1-8. 10.1016/j.prostaglandins.2013.11.001.

43. Riley, P.A. (1997). Melanin. Int J Biochem Cell Biol *29*, 1235-1239. 10.1016/s1357-2725(97)00013-7.

44. White, L.P. (1958). Melanin: a naturally occurring cation exchange material. Nature *182*, 1427-1428. 10.1038/1821427a0.

45. Wheeler, M.H., and Bell, A.A. (1988). Melanins and their importance in pathogenic fungi. Curr Top Med Mycol *2*, 338-387. 10.1007/978-1-4612-3730-3_10.

46. Rhodes, J.C., Polacheck, I., and Kwon-Chung, K.J. (1982). Phenoloxidase activity and virulence in isogenic strains of Cryptococcus neoformans. Infect Immun *36*, 1175-1184. 10.1128/iai.36.3.1175-1184.1982.

47. Kwon-Chung, K.J., Tom, W.K., and Costa, J.L. (1983). Utilization of indole compounds by Cryptococcus neoformans to produce a melanin-like pigment. J Clin Microbiol *18*, 1419-1421. 10.1128/jcm.18.6.1419-1421.1983.

48. Salas, S.D., Bennett, J.E., Kwon-Chung, K.J., Perfect, J.R., and Williamson, P.R. (1996). Effect of the laccase gene CNLAC1, on virulence of Cryptococcus neoformans. J Exp Med *184*, 377-386. 10.1084/jem.184.2.377.

49. Tsai, H.F., Washburn, R.G., Chang, Y.C., and Kwon-Chung, K.J. (1997). Aspergillus fumigatus arp1 modulates conidial pigmentation and complement deposition. Mol Microbiol *26*, 175-183. 10.1046/j.1365-2958.1997.5681921.x.

50. Eisenman, H.C., Nosanchuk, J.D., Webber, J.B., Emerson, R.J., Camesano, T.A., and Casadevall, A. (2005). Microstructure of cell wall-associated melanin in the human pathogenic fungus Cryptococcus neoformans. Biochemistry *44*, 3683-3693. 10.1021/bi047731m.

51. Eisenman, H.C., Mues, M., Weber, S.E., Frases, S., Chaskes, S., Gerfen, G., and Casadevall, A. (2007). *Cryptococcus neoformans* laccase catalyses melanin synthesis from both D- and L-DOPA. Microbiology (Reading) *153*, 3954-3962. 10.1099/mic.0.2007/011049-0.

52. Stappers, M.H.T., Clark, A.E., Aimanianda, V., Bidula, S., Reid, D.M., Asamaphan, P., Hardison, S.E., Dambuza, I.M., Valsecchi, I., Kerscher, B., et al. (2018). Recognition of DHN-melanin by a C-type lectin receptor is required for immunity to *Aspergillus*. Nature *555*, 382-386. 10.1038/nature25974.

53. Tam, J.M., Mansour, M.K., Khan, N.S., Yoder, N.C., and Vyas, J.M. (2012). Use of fungal derived polysaccharide-conjugated particles to probe Dectin-1 responses in innate immunity. Integr Biol (Camb) *4*, 220-227. 10.1039/c2ib00089j.

54. Reedy, J.L., Crossen, A.J., Negoro, P.E., Harding, H.B., Ward, R.A., Vargas-Blanco, D.A., Timmer, K.D., Reardon, C.M., Basham, K.J., Mansour, M.K., et al. (2023). The C-Type Lectin Receptor Dectin-2 Is a Receptor for *Aspergillus fumigatus* Galactomannan. mBio *14*, e0318422. 10.1128/mbio.03184-22.

55. Chow, A.W., Liang, J.F., Wong, J.S., Fu, Y., Tang, N.L., and Ko, W.H. (2010). Polarized secretion of interleukin (IL)-6 and IL-8 by human airway epithelia 16HBE14o- cells in response to cationic polypeptide challenge. PLoS One *5*, e12091. 10.1371/journal.pone.0012091.

56. Pillai, D.K., Sankoorikal, B.J., Johnson, E., Seneviratne, A.N., Zurko, J., Brown, K.J., Hathout, Y., and Rose, M.C. (2014). Directional secretomes reflect polarity-specific

functions in an in vitro model of human bronchial epithelium. Am J Respir Cell Mol Biol *50*, 292-300. 10.1165/rcmb.2013-0188OC.

57. Skronska-Wasek, W., Durlanik, S., Garnett, J.P., and Pflanz, S. (2021). Polarized cytokine release from airway epithelium differentially influences macrophage phenotype. Mol Immunol *132*, 142-149. 10.1016/j.molimm.2021.01.029.

58. Hurley, B.P., Siccardi, D., Mrsny, R.J., and McCormick, B.A. (2004). Polymorphonuclear cell transmigration induced by *Pseudomonas aeruginosa* requires the eicosanoid hepoxilin A3. J Immunol *173*, 5712-5720. 10.4049/jimmunol.173.9.5712.

59. Kusek, M.E., Pazos, M.A., Pirzai, W., and Hurley, B.P. (2014). *In vitro* coculture assay to assess pathogen induced neutrophil trans-epithelial migration. J Vis Exp, e50823. 10.3791/50823.

60. Crossen, A.J., Ward, R.A., Reedy, J.L., Surve, M.V., Klein, B.S., Rajagopal, J., and Vyas, J.M. (2022). Human Airway Epithelium Responses to Invasive Fungal Infections: A Critical Partner in Innate Immunity. J Fungi (Basel) *9*. 10.3390/jof9010040.

61. Chamilos, G., and Carvalho, A. (2020). *Aspergillus fumigatus* DHN-Melanin. Curr Top Microbiol Immunol *425*, 17-28. 10.1007/82_2020_205.

62. Kyrmizi, I., Ferreira, H., Carvalho, A., Figueroa, J.A.L., Zarmpas, P., Cunha, C., Akoumianaki, T., Stylianou, K., Deepe, G.S., Jr., Samonis, G., et al. (2018). Calcium sequestration by fungal melanin inhibits calcium-calmodulin signalling to prevent LC3-associated phagocytosis. Nat Microbiol *3*, 791-803. 10.1038/s41564-018-0167-x.

63. Nosanchuk, J.D., and Casadevall, A. (2003). The contribution of melanin to microbial pathogenesis. Cell Microbiol *5*, 203-223. 10.1046/j.1462-5814.2003.00268.x.

64. Levardon, H., Yonker, L.M., Hurley, B.P., and Mou, H. (2018). Expansion of Airway Basal Cells and Generation of Polarized Epithelium. Bio Protoc *8*. 10.21769/BioProtoc.2877.

65. Mou, H., Vinarsky, V., Tata, P.R., Brazauskas, K., Choi, S.H., Crooke, A.K., Zhang, B., Solomon, G.M., Turner, B., Bihler, H., et al. (2016). Dual SMAD Signaling Inhibition Enables Long-Term Expansion of Diverse Epithelial Basal Cells. Cell Stem Cell *19*, 217-231. 10.1016/j.stem.2016.05.012.

66. Mou, H., Yang, Y., Riehs, M.A., Barrios, J., Shivaraju, M., Haber, A.L., Montoro, D.T., Gilmore, K., Haas, E.A., Paunovic, B., et al. (2021). Airway basal stem cells generate distinct subpopulations of PNECs. Cell Rep *35*, 109011. 10.1016/j.celrep.2021.109011.

67. Rossner, M., and Yamada, K.M. (2004). What's in a picture? The temptation of image manipulation. J Cell Biol *166*, 11-15. 10.1083/jcb.200406019.

Figure 1

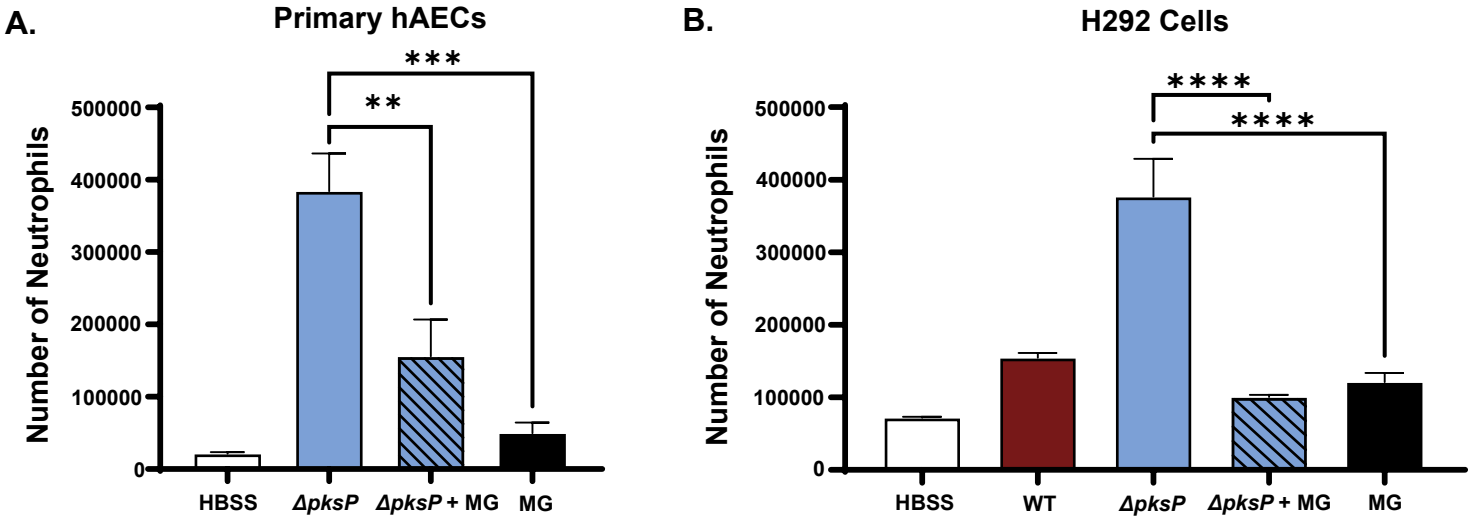
A.
Primary hAECs
***
**
Number of Neutrophils
500000
400000
300000
200000
100000
0
HBSS
ΔpksP
ΔpksP + MG
MG
B.
H292 Cells
****
****
Number of Neutrophils
500000
400000
300000
200000
100000
0
HBSS
WT
ΔpksP
ΔpksP + MG
MG

Figure 2

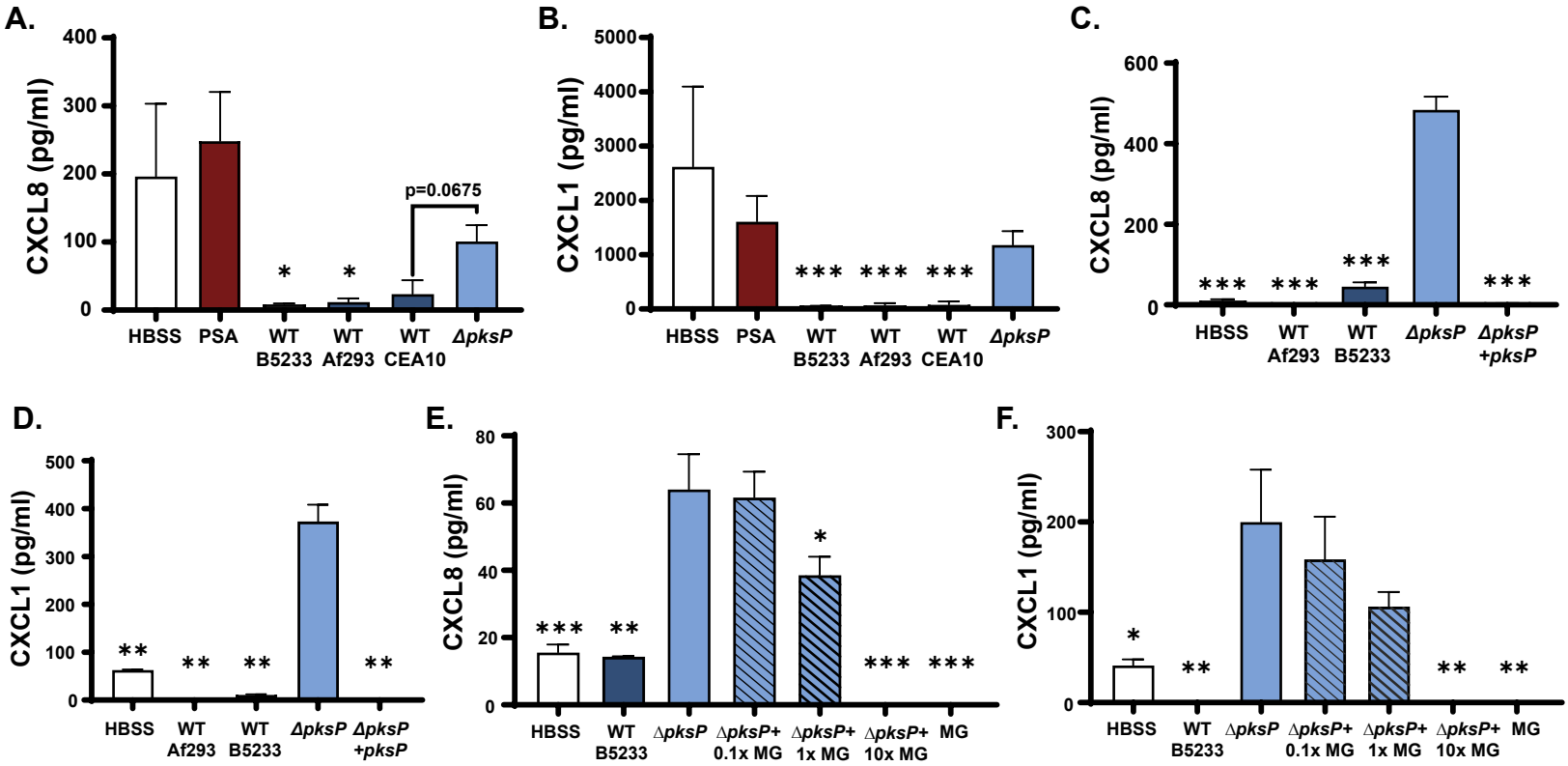
A.
CXCL8 (pg/ml)
400
300
200
100
0
p=0.0675
*
*
HBSS
PSA
WT B5233
WT Af293
WT CEA10
ΔpksP
B.
CXCL1 (pg/ml)
5000
4000
3000
2000
1000
0
***
***
***
HBSS
PSA
WT B5233
WT Af293
WT CEA10
ΔpksP
C.
CXCL8 (pg/ml)
600
400
200
0
***
***
***
***
HBSS
WT Af293
WT B5233
ΔpksP
ΔpksP +pksP
D.
CXCL1 (pg/ml)
500
400
300
200
100
0
**
**
**
**
HBSS
WT Af293
WT B5233
ΔpksP
ΔpksP +pksP
E.
CXCL8 (pg/ml)
80
60
40
20
0
***
**
*
***
***
HBSS
WT B5233
ΔpksP
ΔpksP+ 0.1x MG
ΔpksP+ 1x MG
ΔpksP+ 10x MG
MG
F.
CXCL1 (pg/ml)
300
200
100
0
*
**
**
**
HBSS
WT B5233
ΔpksP
ΔpksP+ 0.1x MG
ΔpksP+ 1x MG
ΔpksP+ 10x MG
MG

Figure 3

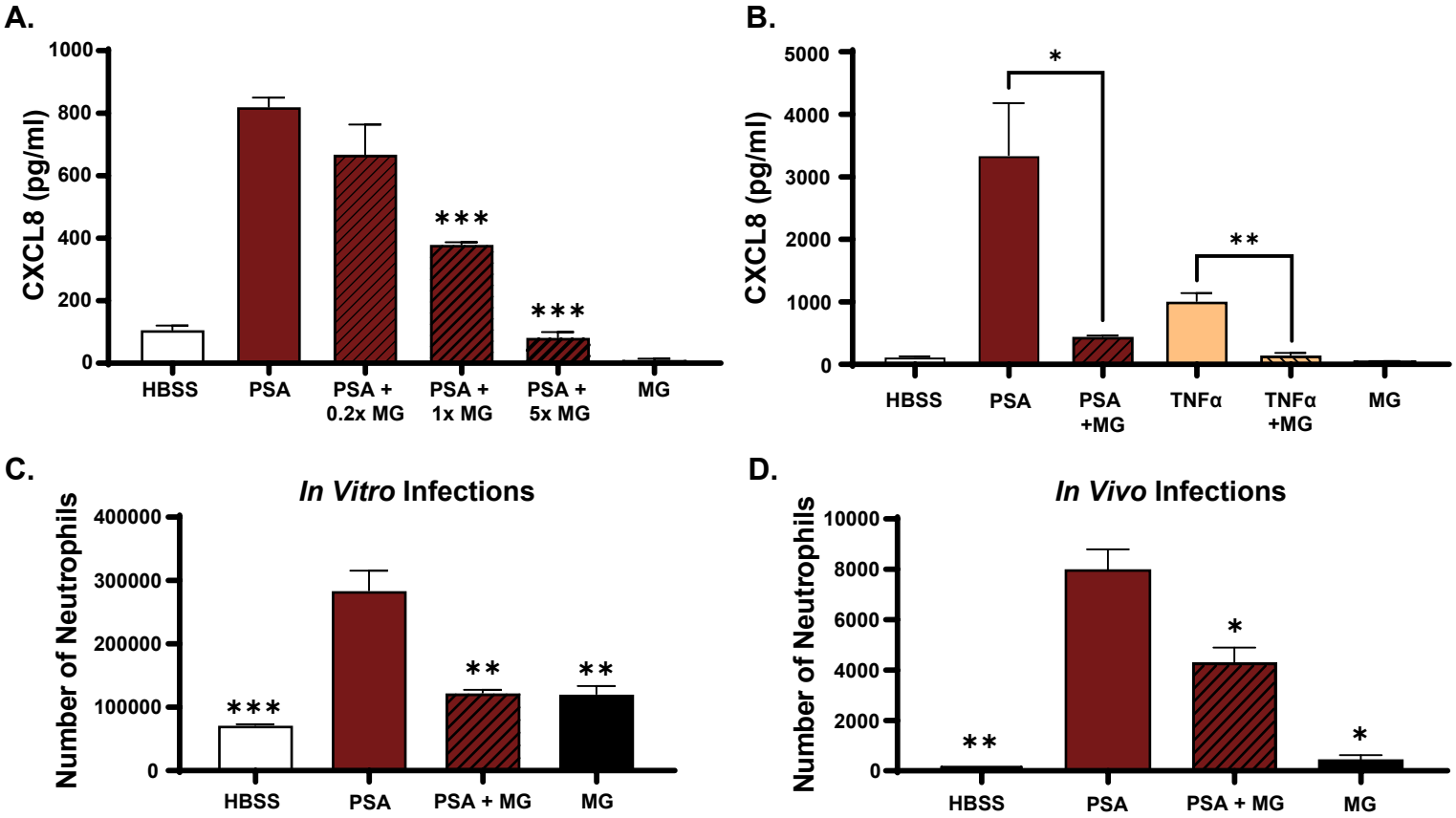
A.
CXCL8 (pg/ml)
1000
800
600
400
200
0
***
***
HBSS
PSA
PSA + 0.2x MG
PSA + 1x MG
PSA + 5x MG
MG
B.
CXCL8 (pg/ml)
5000
4000
3000
2000
1000
0
*
**
HBSS
PSA
PSA +MG
TNFα
TNFα +MG
MG
C.
In Vitro Infections
Number of Neutrophils
400000
300000
200000
100000
0
***
**
**
HBSS
PSA
PSA + MG
MG
D.
In Vivo Infections
Number of Neutrophils
10000
8000
6000
4000
2000
0
**
*
*
HBSS
PSA
PSA + MG
MG

Figure 4

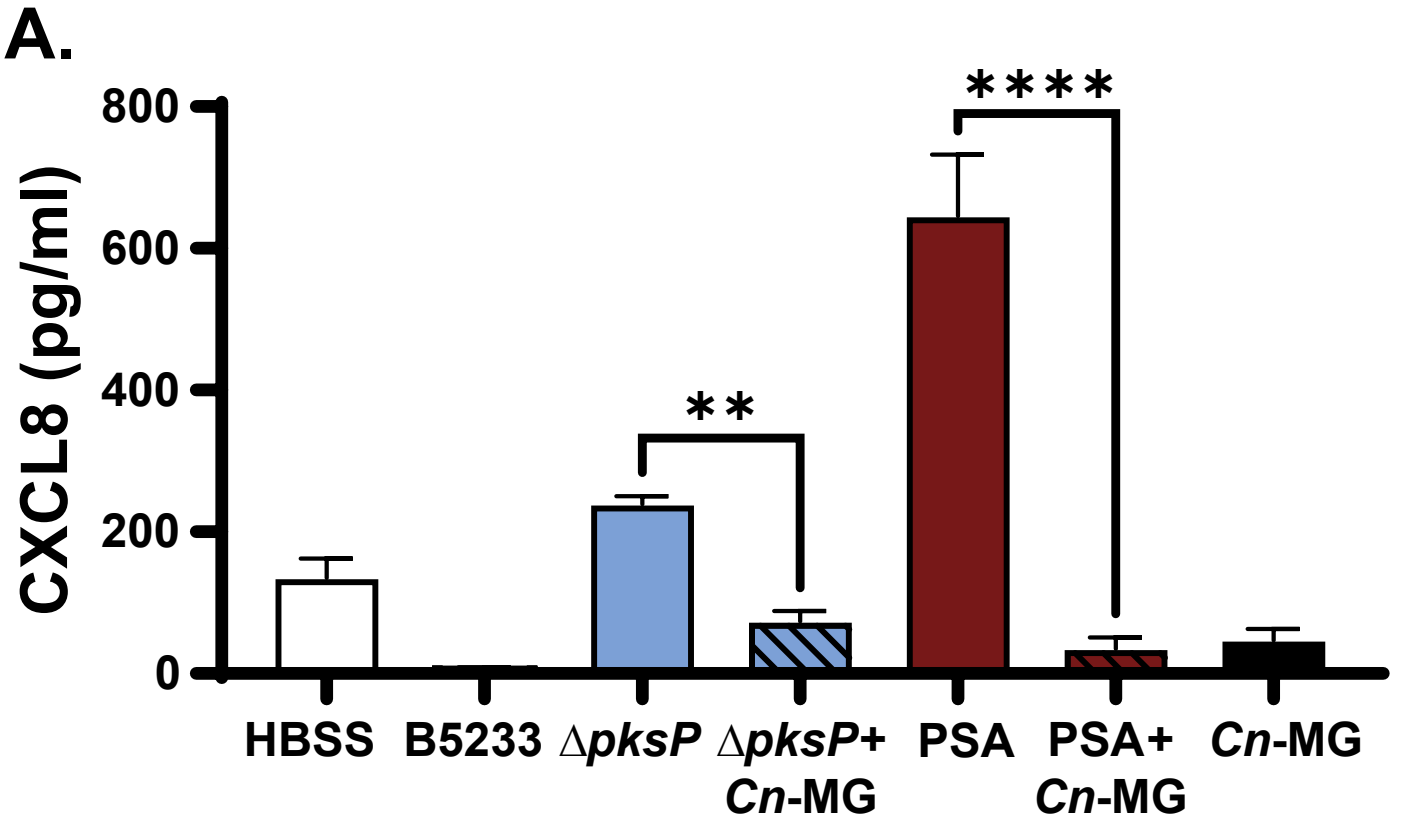
A.
CXCL8 (pg/ml)
800
600
400
200
0
****
**
HBSS
B5233
ΔpksP
ΔpksP+ Cn-MG
PSA
PSA+ Cn-MG
Cn-MG

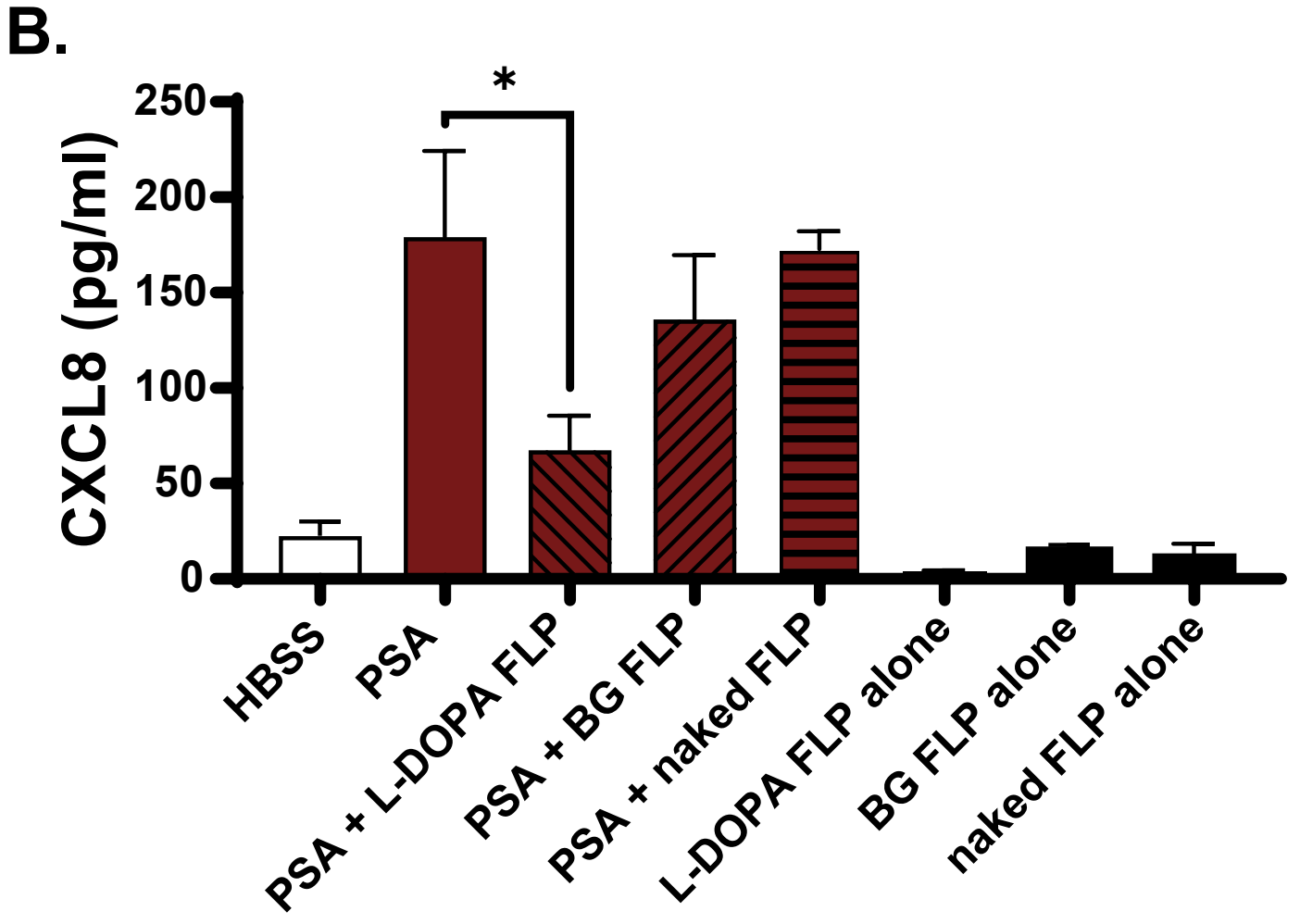
B.
CXCL8 (pg/ml)
250
200
150
100
50
0
*
HBSS
PSA
PSA + L-DOPA FLP
PSA + BG FLP
PSA + naked FLP
L-DOPA FLP alone
BG FLP alone
naked FLP alone

Figure 5

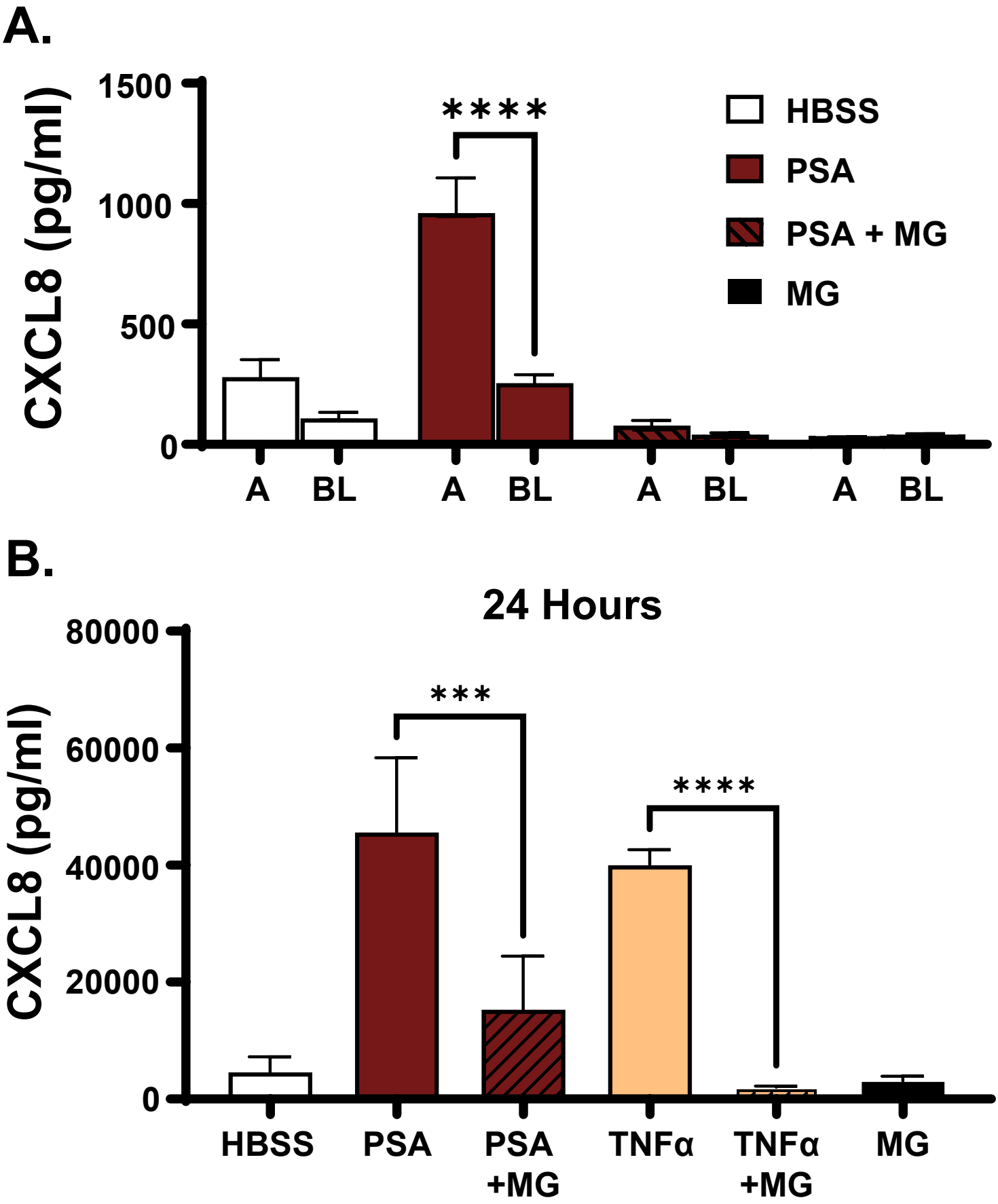
A.
CXCL8 (pg/ml)
1500
1000
500
0
****
HBSS
PSA
PSA + MG
MG
A
BL
A
BL
A
BL
A
BL
B.
24 Hours
CXCL8 (pg/ml)
80000
60000
40000
20000
0
***
****
HBSS
PSA
PSA +MG
TNFα
TNFα +MG
MG

Figure 6

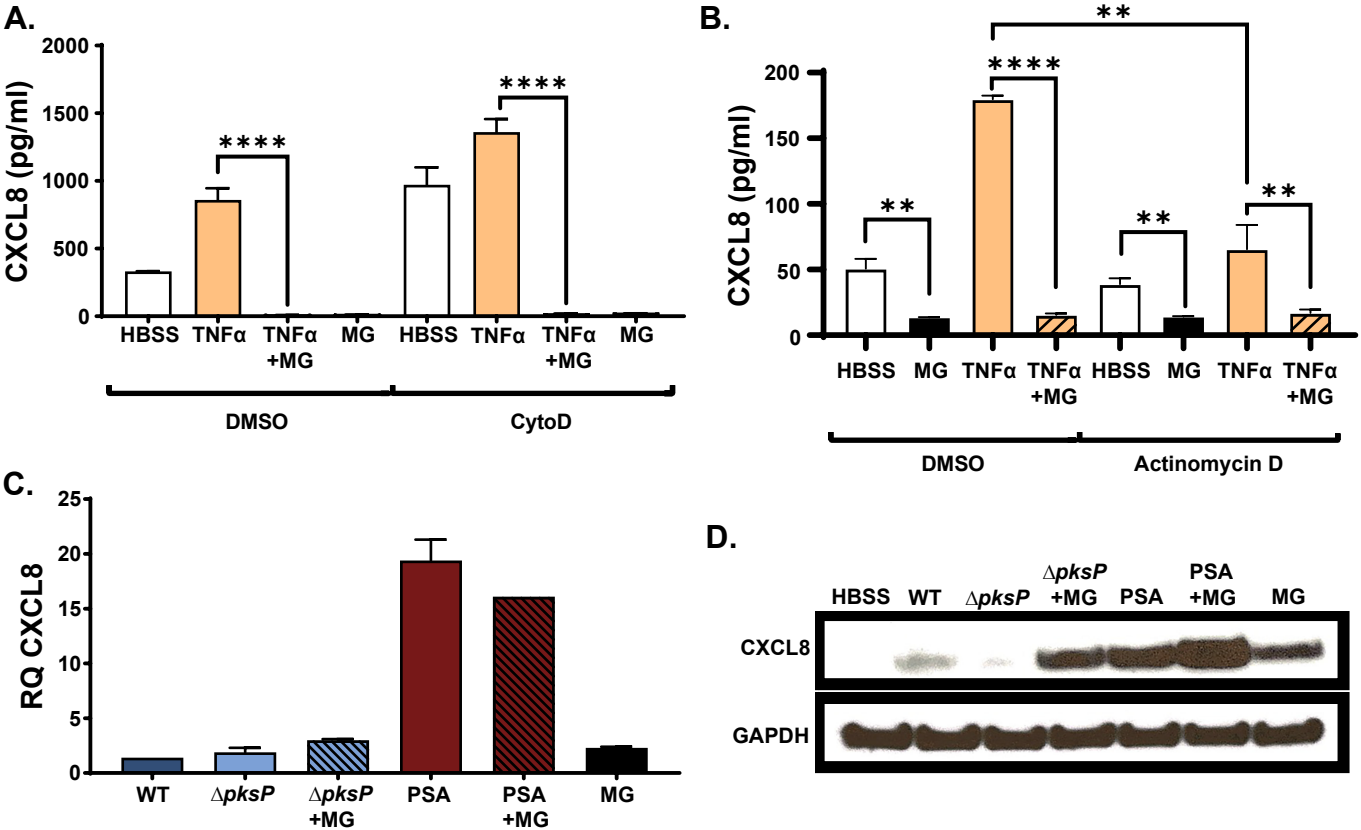
A.
CXCL8 (pg/ml)
2000
1500
1000
500
0
****
****
HBSS
TNFα
TNFα +MG
MG
HBSS
TNFα
TNFα +MG
MG
DMSO
CytoD
B.
CXCL8 (pg/ml)
200
150
100
50
0
**
****
**
**
**
HBSS
MG
TNFα
TNFα +MG
HBSS
MG
TNFα
TNFα +MG
DMSO
Actinomycin D
C.
RQ CXCL8
25
20
15
10
5
0
WT
ΔpksP
ΔpksP +MG
PSA
PSA +MG
MG
D.
HBSS
WT
ΔpksP
ΔpksP +MG
PSA
PSA +MG
MG
CXCL8
GAPDH